doi:10.1093/plcell/koab242

THE PLANT CELL

THE PLANT CELL 2022: 34: 679–697

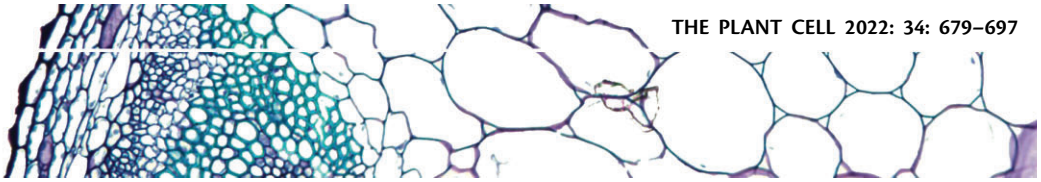

Research Article

The calcium-dependent protein kinase CPK28 is targeted by the ubiquitin ligases ATL31 and ATL6 for proteasome-mediated degradation to fine-tune immune signaling in Arabidopsis

Xiaotong Liu [1,†] **Yuanyuan Zhou** [1,2,†] **Mingshuo Du** [1,2,3] **Xuelian Liang** [3] **Fenggui Fan** [1] **Guozhong Huang** [1] **Yanmin Zou** [1] **Jiaojiao Bai** [1,2] **and Dongping Lu** [1,3,*,‡]

1 State Key Laboratory of Plant Genomics, Center for Agricultural Resources Research, Institute of Genetics and Developmental Biology, Chinese Academy of Sciences, Shijiazhuang, Hebei 050021, China
2 College of Advanced Agricultural Sciences, University of Chinese Academy of Sciences, Beijing 100049, China
3 Hebei Collaboration Innovation Center for Cell Signaling, Hebei Normal University, Shijiazhuang 050024, China

*Author for correspondence: dplu@sjziam.ac.cn
†These authors contributed equally (X.Liu., Y.Z.).
‡Senior author.

X.Liu., Y.Z., M.D., and D.L. designed the study. X.Liu., Y.Z., M.D., X.L., F.F., G.H., and J.B. performed the experiments. X.Liu., Y.Z., M.D., Y.Zou., and D.L. analyzed the data. D.L. and X.Liu. wrote the paper.

The author responsible for distribution of materials integral to the findings presented in this article in accordance with the policy described in the Instructions for Authors (https://academic.oup.com/plcell) is: Dongping Lu (dplu@sjziam.ac.cn).

Abstract

Immune responses are triggered when pattern recognition receptors recognize microbial molecular patterns. The Arabidopsis (*Arabidopsis thaliana*) receptor-like cytoplasmic kinase BOTRYTIS-INDUCED KINASE1 (BIK1) acts as a signaling hub of plant immunity. BIK1 homeostasis is maintained by a regulatory module in which CALCIUM-DEPENDENT PROTEIN KINASE28 (CPK28) regulates BIK1 turnover via the activities of two E3 ligases. Immune-induced alternative splicing of *CPK28* attenuates CPK28 function. However, it remained unknown whether CPK28 is under proteasomal control. Here, we demonstrate that CPK28 undergoes ubiquitination and 26S proteasome-mediated degradation, which is enhanced by flagellin treatment. Two closely related ubiquitin ligases, ARABIDOPSIS TÓXICOS EN LEVADURA31 (ATL31) and ATL6, specifically interact with CPK28 at the plasma membrane; this association is enhanced by flagellin elicitation. ATL31/6 directly ubiquitinate CPK28, resulting in its proteasomal degradation. Furthermore, ATL31/6 promotes the stability of BIK1 by mediating CPK28 degradation. Consequently, ATL31/6 positively regulate BIK1-mediated immunity. Our findings reveal another mechanism for attenuating CPK28 function to maintain BIK1 homeostasis and enhance immune responses.

Introduction

Plants have a sophisticated innate immune system to defend against pathogen invasion. Microbe-associated molecular patterns or pathogen-associated molecular patterns (PAMPs) trigger immune responses in plants, a process known as pattern-triggered immunity (PTI). PTI confers the host defense against a wide range of phytopathogens (Jones and

Received April 02, 2021. Accepted September 22, 2021. Advance access publication October 1, 2021

IN A NUTSHELL

Background: Plants rely on innate immunity to thwart off microbial pathogens. Immune responses are triggered when immune receptors recognize microbial molecular patterns. The cytoplasmic kinase BOTRYTIS-INDUCED KINASE 1 (BIK1) plays a central role in relaying signals from multiple upstream immune receptors to diverse substrate proteins. The homeostasis of BIK1 is tightly controlled and is maintained by a regulatory module, in which the calcium-dependent protein kinase CPK28 contributes to BIK1 turnover.

Question: Are CPK28 proteins under further control to maintain BIK1 homeostasis and fine-tune immune signaling?

Findings: We found that CPK28 proteins undergo a type of modification called ubiquitination that serves as a signal for protein degradation via the 26S proteasome machinery. Interestingly, the bacterial flagellin treatment enhances the ubiquitination and degradation of CPK28 proteins. Two ubiquitin ligases, ARABIDOPSIS TÓXICOS EN LEVADURA 31 (ATL31) and ATL6 directly interact with and mediate the ubiquitination of CPK28, which results in the proteasomal degradation of CPK28 and attenuation of CPK28 function. Therefore, ATL31 and ATL6 modulate BIK1 homeostasis and regulate immune signaling via mediating CPK28 degradation. Our work reveals how CPK28 is kept in check to maintain BIK1 homeostasis and to enhance immune responses.

Next steps: We aim to investigate how signals are relayed from immune receptors to ATL31 and ATL6 to mediate the degradation of CPK28.

Dangl, 2006). In Arabidopsis (*Arabidopsis thaliana*), the bacterial flagellin or its derived peptide flg22 is recognized by FLAGELLIN-SENSING2 (FLS2), a well-studied plasma membrane-localized leucine-rich repeat receptor kinase (LRR-RK; Gomez-Gomez and Boller, 2000). BRI1-ASSOCIATED RECEPTOR KINASE1 (BAK1) serves as a co-receptor for FLS2 and other pattern recognition receptors (PRRs), such as EF-TU RECEPTOR (EFR), which perceives the bacterial elongation factor EF-Tu and the derived epitope elf18. Upon ligand binding, FLS2 and EFR rapidly interact with BAK1 and the related SOMATIC-EMBRYOGENESIS RECEPTOR-LIKE KINASE proteins to activate downstream immune signaling (Zipfel et al., 2006; Chinchilla et al., 2007; Heese et al., 2007; Roux et al., 2011). Additionally, PRRs sense endogenous damage-associated molecular patterns that are released upon wounding or pathogen perception (Zipfel, 2014). Arabidopsis PLANT ELICITOR PEPTIDEs (Peps) are perceived by two LRR-RKs, PEP RECEPTOR1 (PEPR1) and PEPR2, triggering immune responses (Yamaguchi et al., 2006, 2010; Krol et al., 2010).

BOTRYTIS-INDUCED KINASE 1 (BIK1) is a receptor-like cytoplasmic kinase (RLCK) that associates with multiple PRRs and functions as a signaling hub immediately downstream of these PRRs. BIK1 undergoes hyperphosphorylation upon PAMP perception in a BAK1-depdendent manner (Lu et al., 2010; Zhang et al., 2010). To date, various substrates have been identified for BIK1. BIK1 directly phosphorylates a plasma membrane-resident NADPH oxidase, RESPIRATORY BURST OXIDASE HOMOLOG D (RbohD), resulting in reactive oxygen species (ROS) burst and stomatal immunity (Kadota et al., 2014; Li et al., 2014). In addition, BIK1 phosphorylates the Ca^{2+}-permeable channel OSCA1.3 within minutes of flg22 treatment and enhances its channel activity, which is critical for PAMP-induced stomatal closure during immunity (Thor et al., 2020). Upon pathogen attack, BIK1 also phosphorylates and activates two CYCLIC NUCLEOTIDE-GATED CHANNEL (CNGC) proteins, CNGC2 and CNGC4, which triggers calcium entry into the cytosol (Tian et al., 2019).

Immune signaling is finely tuned to ensure its appropriate magnitude and duration. BAK1-INTERACTING RECEPTOR-LIKE KINASE2 (BIR2) and BIR3 block the association of FLS2 with BAK1 in the resting state, whereas they are released from BAK1 after flg22 perception, facilitating the interaction between BAK1 and FLS2 (Halter et al., 2014; Imkampe et al., 2017). Protein Ser/Thr phosphatase 2A (PP2A) negatively regulates immunity by dephosphorylating BAK1 (Segonzac et al., 2014). Some endogenous peptides, such as RAPID ALKALINIZATION FACTOR23 (RALF23) and RALF33, are rapidly released and bind to their receptor FERONIA (FER) to inhibit immunity in Arabidopsis (Stegmann et al., 2017). Another Arabidopsis RLCK, AvrPphB SUSCEPTIBLE1-LIKE13 (PBL13), phosphorylates the C terminus of RbohD to affect its activity and stability, thereby negatively regulating immunity (Lin et al., 2015; Lee et al., 2020). The transcription factors TARGET OF EAT1 (TOE1) and TOE2 directly bind to the *FLS2* promoter and inhibit its activity to suppress plant immunity during the early stages of seedling development (Zou et al., 2018, 2020).

Protein ubiquitination is a widespread type of post-translational modification that is involved in the regulation of signal transduction. In the presence of ATP, ubiquitin is activated and transferred to a specific target protein in a stepwise manner by three types of enzymes: ubiquitin activating enzyme (UBA, E1), ubiquitin conjugating enzyme (UBC, E2), and ubiquitin ligase (E3). During ubiquitination, E3 ubiquitin ligases play a critical role in determining the substrate specificity. A major consequence of ubiquitination is the targeting of the substrate proteins to the 26S proteasome for degradation (Callis, 2014). Ubiquitination plays an important role in regulating immune signaling. FLS2 is ubiquitinated by two ubiquitin ligases PLANT U-BOX12 (PUB12) and PUB13, which leads to the attenuation of immune

signaling (Lu et al., 2011). The ubiquitination of RbohD by PBL13 INTERACTING RING DOMAIN E3 LIGASE is further enhanced upon RbohD phosphorylation catalyzed by PBL13, which results in the degradation of RbohD and the negative regulation of immune signaling (Lee et al., 2020). PUB22 ubiquitinates EXOCYST SUBUNIT 70 PROTEIN B2 (Exo70B2), a subunit of the exocyst complex required for activation of immune responses, leading to the degradation of Exo70B2 and the attenuation of immune signaling (Stegmann et al., 2012; Furlan et al., 2017).

The immune signaling hub BIK1 is subjected to tight regulation. BIK1 homeostasis is maintained by a regulatory module that consists of CALCIUM-DEPENDENT PROTEIN KINASE28 (CPK28), two closely related ubiquitin ligases (PUB25 and PUB26), and heterotrimeric G proteins. In this module, PUB25/26 ubiquitinate BIK1, leading to its degradation. The ligase activity of PUB25 is enhanced when it is phosphorylated at Thr95 by CPK28, which promotes the polyubiquitination and degradation of BIK1 (Monaghan et al., 2014; Wang et al., 2018).

It was recently reported that a retained intron (RI) variant of *CPK28*, known as *CPK28*-RI, is induced after treatment with flg22 (Bazin et al., 2020) or AtPeps (Dressano et al., 2020). *CPK28*-RI encodes a truncated CPK28 isoform that exhibits impaired kinase activity (Dressano et al., 2020). The immune-induced alternative splicing of the *CPK28* transcripts plays a regulatory role in dynamically amplifying immune signaling (Bazin et al., 2020; Dressano et al., 2020). Furthermore, a more recent proteomics study showed that CPK28 is ubiquitinated at multiple Lys residues (Grubb et al., 2021). However, the underlying mechanisms of CPK28 ubiquitination and whether CPK28 undergoes proteasomal degradation to maintain immune homeostasis remained unknown.

Here, we demonstrate that CPK28 undergoes ubiquitination and 26S proteasome-mediated degradation that are enhanced by flg22 stimulation. Two closely related ubiquitin ligases, ARABIDOPSIS TÓXICOS EN LEVADURA 31 (ATL31) and ATL6, interact with CPK28 in an flg22-enhanced manner. Furthermore, ATL31 and ATL6 directly ubiquitinate CPK28, resulting in the proteasomal degradation of CPK28. As a result, ATL31 and ATL6 positively regulate BIK1 stability and immune responses. Our work reveals how CPK28 is targeted by ATL31/6 for proteasome-mediated degradation to maintain BIK1 homeostasis and dynamically regulate immune signaling.

Results

CPK28 undergoes ubiquitination and 26S proteasome-mediated degradation

CPK28 is a key component of the recently characterized immune regulatory module that modulates BIK1 stability (Monaghan et al., 2014; Wang et al., 2018). To examine whether CPK28 is under proteolytic control to keep this regulatory module in check, we examined its ubiquitination and proteasomal degradation. We performed *in vivo* ubiquitination assays by transiently expressing ubiquitin tagged with the FLAG epitope (FLAG-Ub) and CPK28 tagged with hemagglutinin (CPK28-HA) in Arabidopsis protoplasts; a similar approach was previously used to examine the ubiquitination of BIK1 (Ma et al., 2020) and FLS2 (Lu et al., 2011) *in vivo*. Following immunoprecipitation (IP) with anti-FLAG antibodies, the ubiquitinated CPK28 proteins were detected by immunoblotting with anti-HA antibodies. CPK28 exhibited ladder-like smears, which are indicative of protein ubiquitination (Figure 1A). Notably, a recent proteomics study identified multiple ubiquitination sites on CPK28 proteins (Grubb et al., 2021), suggesting that CPK28 indeed undergoes ubiquitination. Furthermore, we found that the ubiquitination of CPK28 was enhanced by flg22 treatment (Figure 1A).

In addition to CPK28, other negative immune regulators, such as BIR2 and BIR3, also undergo ubiquitination (Supplemental Figure S1, A and B); consistently, ubiquitination sites were also identified on both BIR2 and BIR3 by the recent proteomics study (Grubb et al., 2021). However, ubiquitination of PBL13 and RCN1 (PP2A subunit A1) was not observed under the conditions we used (Supplemental Figure S1, C and D), demonstrating the specificity of this *in vivo* ubiquitination system.

We then examined the turnover of CPK28 protein. We raised antibodies that specifically detected CPK28 in Col-0 but not in *cpk28* mutants (Monaghan et al., 2014; Supplemental Figure S2, A–E). The anti-CPK28 antibodies specifically recognized recombinant CPK28 proteins, but not other tested CPKs, such as CPK8, CPK6, CPK1, CPK3, and CPK16 that is closely related to CPK28 (Boudsocq and Sheen, 2013; Supplemental Figure S2F). Importantly, the anti-CPK28 antibodies did not recognize recombinant CPK28-RI proteins (Supplemental Figure S2G). CPK28 protein accumulation increased in Col-0 seedlings treated with the 26S proteasome inhibitor MG132, as measured by immunoblotting with anti-CPK28 antibodies (Supplemental Figure S3A). Moreover, when Col-0 seedlings were treated with cycloheximide (CHX) to block protein synthesis, CPK28 protein accumulation declined over time. However, the decrease in CPK28 protein level was largely blocked by MG132 treatment (Figure 1B), suggesting that CPK28 proteins are under proteasomal control. Notably, in the presence of CHX, we observed a significant reduction in CPK28 protein levels within 2 h after flg22 treatment. This degradation was inhibited by MG132 treatment (Figure 1C), indicating that flg22 treatment enhances the proteasomal degradation of CPK28. Moreover, like CPK28, both BIR2 and BIR3 also undergo proteasomal degradation, as assayed using proteins transiently expressed in Arabidopsis protoplasts (Supplemental Figure S3, B and C).

Identification of ubiquitin ligases that mediate CPK28 degradation

We then sought to identify E3 ubiquitin ligases that mediate the ubiquitination of CPK28. Considering that the interaction between ubiquitin ligase and its target may result in

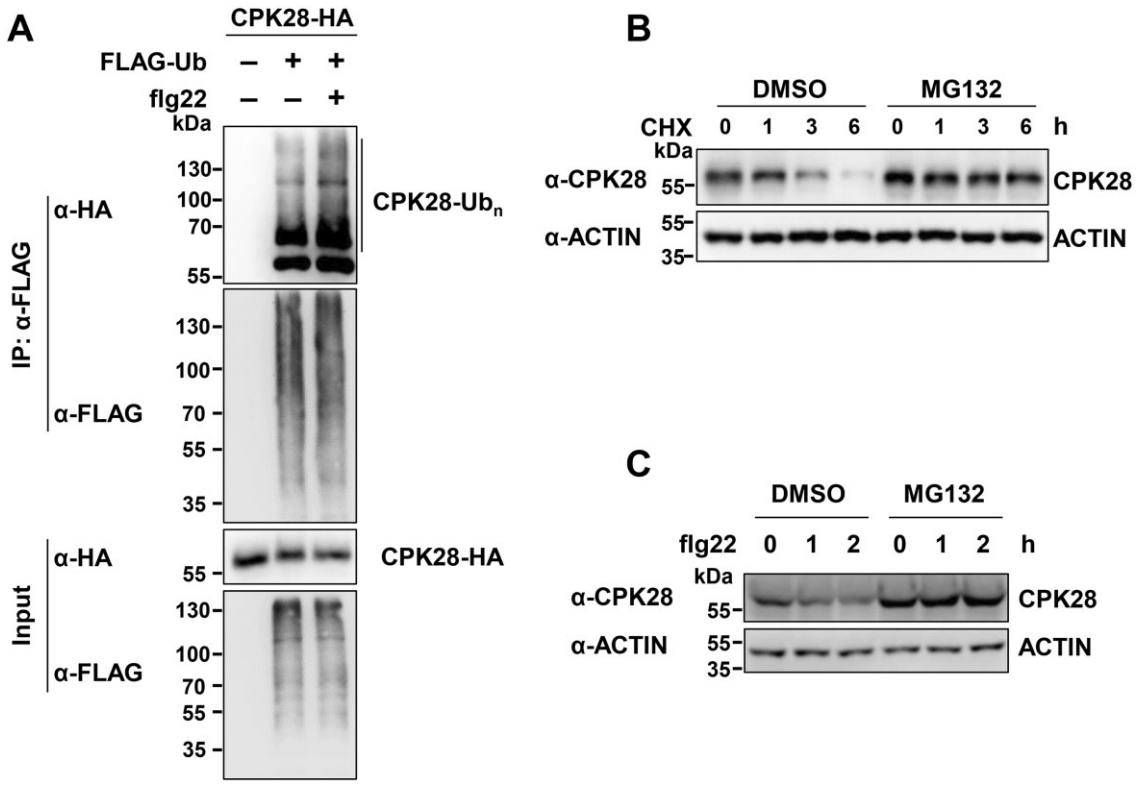

Figure 1 CPK28 undergoes ubiquitination and 26S proteasome-mediated degradation. A, flg22 treatment enhances CPK28 ubiquitination *in vivo*. FLAG-Ub and CPK28-HA were co-expressed in Arabidopsis protoplasts. In the presence of 20-μM MG132, the protoplasts were treated with 2-μM flg22 for 30 min before harvesting. Total ubiquitinated proteins were immunoprecipitated with anti-FLAG antibodies, and ubiquitinated CPK28 proteins were detected by immunoblotting with anti-HA antibodies. B, CPK28 undergoes proteasomal degradation. Seven-day-old Col-0 seedlings (10 seedlings per sample) were treated with 100-μM CHX for the indicated times in the presence or absence of 50-μM MG132. Total proteins were isolated from whole seedlings. CPK28 proteins were detected with anti-CPK28 antibodies. ACTIN was used as a loading control. C, flg22 treatment enhances the proteasomal degradation of CPK28. Seven-day-old Col-0 seedlings (10 seedlings per sample) were treated with 100-μM CHX in the presence or absence of 50-μM MG132, followed 1 h later by treatment with 2-μM flg22 for the indicated times. Total proteins were isolated from whole seedlings. CPK28 proteins were detected with anti-CPK28 antibodies. ACTIN was used as a loading control.

degradation of the target protein, instead of directly screening for CPK28 interactors, we used an alternative approach to identify the cognate ubiquitin ligases of CPK28. We performed RNA sequencing (RNA-seq) to identify ubiquitin ligase genes that were differentially expressed upon flg22 treatment using RNA isolated from Arabidopsis seedlings treated with flg22 or water (Supplemental Figure S4A). Forty-nine ubiquitin ligase genes were upregulated upon flg22 treatment, and 22 were downregulated (Supplemental Figure S4B and Supplemental Table S1), and their expression was confirmed by reverse transcription- quantitative polymerase chain reaction (RT-qPCR; Supplemental Figure S4C).

To examine which ubiquitin ligases could mediate the degradation of CPK28, we performed a leaf protoplast cell-based screen by co-expressing *CPK28* together with a selected ubiquitin ligase gene. To validate the feasibility of this screening strategy, we co-expressed *PUB25-HA* together with *BIK1-FLAG* in protoplasts, using a green fluorescent protein (GFP)-FLAG fusion as a transfection control. Consistent with a previous report (Wang et al., 2018), *PUB25* overexpression led to the reduced accumulation of BIK1 in this transient system (Supplemental Figure S5). As flg22 enhanced the ubiquitination and proteasomal degradation of CPK28, we screened the flg22-induced ubiquitin ligase genes. We screened 16 of the ubiquitin ligase genes described above and found that the expression of *ATL31-HA* significantly reduced CPK28-MYC protein abundance (Supplemental Figure S6).

ATL31 is a RING-H2 ubiquitin ligase with a well-characterized role in plant carbon/nitrogen (C/N)-nutrient responses (Sato et al., 2009, 2011; Yasuda et al., 2017). ATL31 contains a transmembrane domain at its N terminus. ATL31-GFP proteins were mainly localized to the cell periphery when introduced into onion (*Allium cepa*) epidermal cells (Sato et al., 2009), and ATL31-GFP co-localized with the integral plasma membrane protein BRASSINOSTEROID INSNESITIVE1 (BRI1) fused with red fluorescent protein (RFP; Wang et al., 2001) at the plasma membrane, when these two proteins were co-expressed in Arabidopsis protoplasts (Supplemental Figure S7), suggesting that ATL31 is localized to the plasma membrane in this expression system.

We also analyzed the expression patterns of *ATL31 and CPK28* in response to flg22 treatment. *CPK28* has a canonically spliced transcript and the *CPK28*-RI splice variant

(Dressano et al., 2020; Bazin et al., 2020). The proportion of *CPK28*-RI transcript levels but not those of *CPK28* significantly increased after AtPep1 treatment (Dressano et al., 2020). We found that when the seedlings were treated with flg22, *CPK28* transcript levels started to increase after 15 min of treatment, peaked at 30 min (~16-fold), and returned to the initial level after 120 min (Supplemental Figure S8, A and D). In contrast, *CPK28*-RI transcript levels increased to a peak after 15 min of flg22 treatment (~49-fold), and then decreased to the initial level after 60 min (Supplemental Figure S8, B and D). These results demonstrate that induction of *CPK28* by flg22 was weaker and slower than that of *CPK28*-RI. Moreover, the expression pattern of *ATL31* after flg22 treatment was more similar to that of *CPK28* than to that of *CPK28*-RI (Supplemental Figure S8, A–C).

ATL31/6 interact with CPK28 at the plasma membrane

To examine whether ATL31 interacts with CPK28, we performed co-IP assays in which we co-expressed *CPK28-HA and* $ATL31^{C143H145A}$*-FLAG* in Arabidopsis protoplasts. $ATL31^{C143H145A}$ is an ATL31 variant in which both Cys-143 (Sato et al., 2009) and His-145 in the RING domain were replaced by Ala to impair its activity and decrease the potential target degradation. CPK28-HA associated with $ATL31^{C143H145A}$-FLAG in this assay (Figure 2A). Similarly, $ATL31^{C143H145A}$-HA was also present in the CPK28-FLAG immunoprecipitates (Figure 2B). Importantly, we observed that flg22 treatment enhanced the association of $ATL31^{C143H145A}$ and CPK28 (Figure 2, A and B). Moreover, the association of CPK28 with $ATL31^{C143H145A}$ was much stronger than its association with wild-type (WT) ATL31 (Figure 2C), perhaps mainly due to the degradation of CPK28 mediated by ATL31. To examine whether the association of ATL31 and CPK28 is dependent on the FLS2-BAK1 receptor complex, we performed co-IP using protoplasts isolated from *fls2 and bak1*. ATL31 still associated with CPK28 in both *fls2 and bak1* plants. However, the flg22-enhanced association between ATL31 and CPK28 was no longer observed in the *fls2* or *bak1* mutant (Figure 2, D and E). These results indicate that the association of ATL31 and CPK28 occurs before and after flg22 treatment but is further enhanced upon the recognition of flg22 by the FLS2–BAK1 complex.

ATL6 has the highest level of amino acid sequence similarity with ATL31 (Sato et al., 2009). CPK28 also associated with ATL6, but not with ATL2 (Figure 2, F and G), another ATL family member that was previously shown to be involved in plant defense responses (Serrano and Guzman, 2004). Moreover, flg22 treatment enhanced the association of CPK28 and ATL6 (Figure 2F). Finally, ATL31 was not associated with CPK8, another CPK family member (Supplemental Figure S9). These results demonstrate the specificity of the association between ATL31/6 and CPK28.

CPK28 associates with the plasma membrane via its myristoylation (Monaghan et al., 2014). Therefore, the $CPK28^{G2A}$ variant containing a mutation in its myristoylation site loses its plasma membrane localization when transiently expressed in *Nicotiana benthamiana* (Monaghan et al., 2014). Consistently, the loss of plasma membrane localization of $CPK28^{G2A}$ was also observed in Arabidopsis protoplasts (Supplemental Figure S10). Accordingly, a co-IP assay showed that ATL31 was no longer associated with $CPK28^{G2A}$ (Figure 3A). We also performed bimolecular fluorescence complementation (BiFC) assays in Arabidopsis protoplasts using $ATL31^{C143H145A}$ tagged with the N-terminal half of yellow fluorescent protein (nYFP) tag and CPK28 tagged with the C-terminal half of YFP (cYFP) tag. $ATL31^{C143H145A}$ associated with CPK28 at the plasma membrane (Figure 3B). In line with a previous report (Huang et al., 2019), the plasma membrane-associated protein PCRK1 (pattern-triggered immunity compromised RLCK1; Kong et al., 2016) associated with the plasma membrane-resident protein BRI1 (Wang et al., 2001; Figure 3B). However, $ATL31^{C143H145A}$ did not associate with PCRK1, and CPK28 did not associate with BRI1. Consistently, the CPK28 mutant $CPK28^{G2A}$ did not associate with $ATL31^{C143H145A}$ in the BiFC assays (Figure 3B). These results further confirm the specificity of the association between ATL31 and CPK28 at the plasma membrane.

Furthermore, CPK28 was pulled down by the intracellular region of ATL31 ($ATL31^{\triangle TM}$, amino acids 67–368, lacking the transmembrane domain) and by ATL6 ($ATL6^{\triangle TM}$, amino acids 71–368) fused to a maltose-binding protein (MBP) tag in MBP pull-down (PD) assays (Figure 3C). These results suggest that ATL31/6 directly interact with CPK28.

ATL31/6 ubiquitinate CPK28

ATL31/6 were shown to have ubiquitin ligase activity (Sato et al., 2009; Maekawa et al., 2012). To investigate their roles in CPK28 ubiquitination, we isolated the *ATL31 and ATL6* null mutants, *atl31 and atl6* (Sato et al., 2009, 2011), and generated the homozygous *atl31 atl6* double mutant (Sato et al., 2009, 2011; Supplemental Figure S11, A–F). *atl31 atl6* was slightly smaller than Col-0, but was morphologically very similar to Col-0 during vegetative growth and after the transition from the vegetative to the reproductive stage (Supplemental Figure S11G). CPK28-HA and FLAG-Ub were co-expressed in protoplasts isolated from *atl31 atl6* or Col-0 plants, and the ubiquitination of CPK28 was weaker in *atl31 atl6* than in Col-0 plants (Figure 4A). Notably, CPK28 still underwent ubiquitination even in *atl31 atl6* plants, suggesting that in addition to ATL31/6, there are likely other unidentified ubiquitin ligases involved in CPK28 ubiquitination (Figure 4A).

To further confirm the ubiquitination of CPK28 by ATL31/6, we transfected Col-0 protoplasts with *FLAG-Ub*, *CPK28-HA*, and *ATL31-GFP* or $ATL31^{C143H145A}$*-GFP* and then performed IP with anti-FLAG antibodies. CPK28 was ubiquitinated, and ATL31 overexpression enhanced its ubiquitination (Supplemental Figure S12). Additionally, WT ATL31 underwent substantial autoubiquitination, whereas the

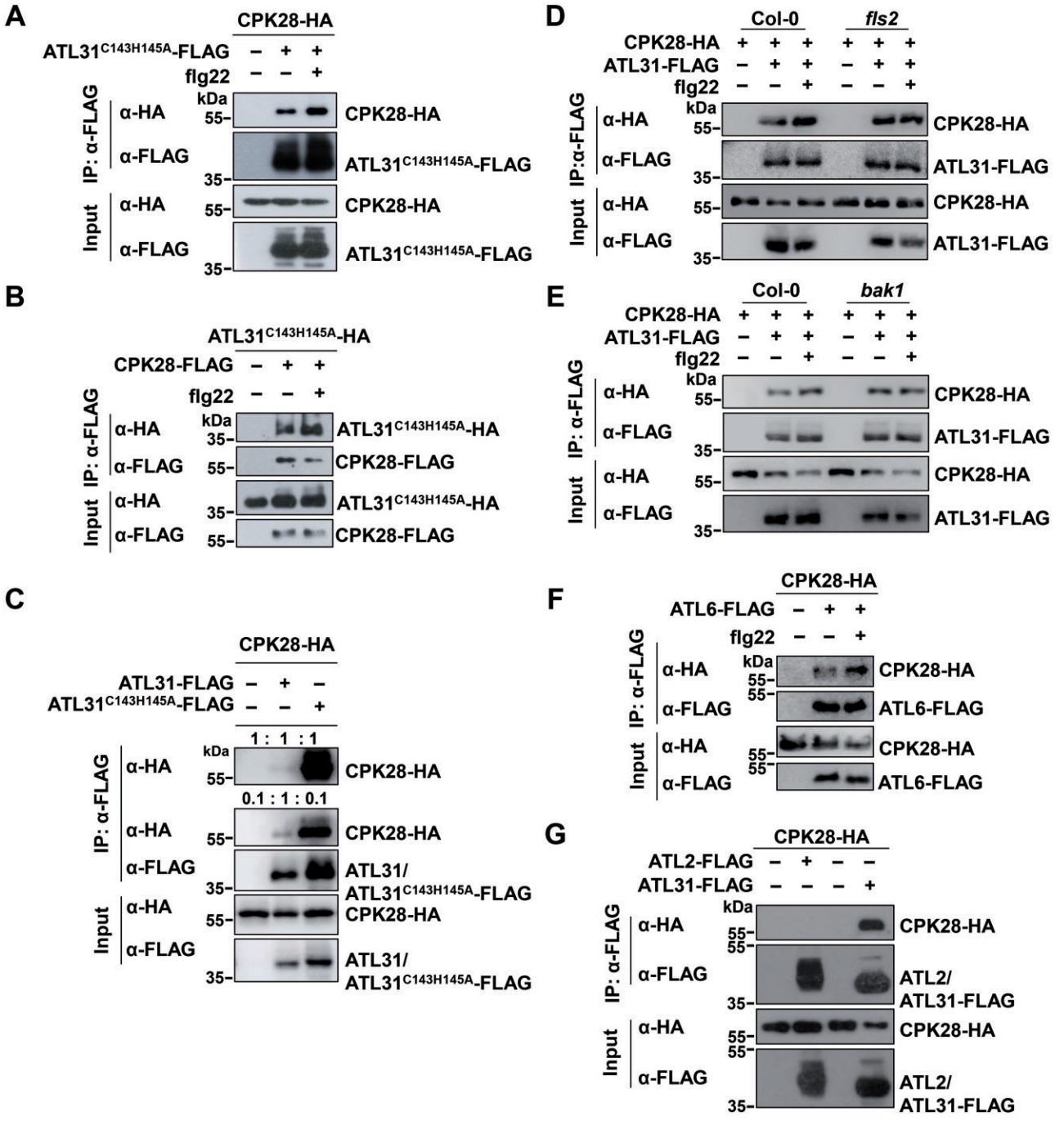

Figure 2 Both ATL31 and ATL6 associate with CPK28. A, flg22 treatment enhances the association of the ATL31^{C143H145A}-FLAG variant and CPK28-HA. CPK28-HA and ATL31^{C143H145A}-FLAG were co-expressed in Arabidopsis protoplasts, and the protoplasts were treated with 2-μM flg22 for 30 min before harvesting. IPs were performed using anti-FLAG antibodies. The immunoprecipitated ATL31^{C143H145A}-FLAG proteins were detected by immunoblotting with anti-FLAG antibodies, and the associated proteins were detected by immunoblotting with anti-HA antibodies (top two parts). The levels of ATL31^{C143H145A}-FLAG and CPK28-HA are shown in the bottom two parts. B, flg22 treatment enhances the association of the ATL31^{C143H145A}-HA variant and CPK28-FLAG. CPK28-FLAG and ATL31^{C143H145A}-HA were co-expressed in Arabidopsis protoplasts, and the protoplasts were treated with 2-μM flg22 for 30 min before harvesting. C, The association of CPK28 with the ATL31^{C143H145A} variant was much stronger than that with WT ATL31. WT ATL31-FLAG or the ATL31^{C143H145A}-FLAG variant was co-expressed with CPK28-HA in Arabidopsis protoplasts. IPs were performed with anti-FLAG antibodies. In the top part, equal amounts of immunoprecipitates were loaded (1:1:1); in the second part, the ATL31^{C143H145A}-FLAG immunoprecipitate and control sample were diluted 10-fold (0.1:1:0.1). The associated CPK28-HA proteins were detected by immunoblotting with anti-HA antibodies. D, E, The association of ATL31 and CPK28 in the *fls2* and *bak1* mutants. ATL31-FLAG was co-expressed with CPK28-HA in protoplasts isolated from Col-0, *fls2*, or *bak1-4* plants. F, flg22 treatment enhances the association of CPK28 and ATL6. ATL6-FLAG was co-expressed with CPK28-HA in protoplasts, and the protoplasts were treated with 2-μM flg22 for 30 min before harvesting. G, CPK28 does not associate with ATL2. ATL2-FLAG was co-expressed with CPK28-HA in protoplasts. D–G, IPs were performed using anti-FLAG antibodies, and the associated proteins were detected by immunoblotting with anti-HA antibodies.

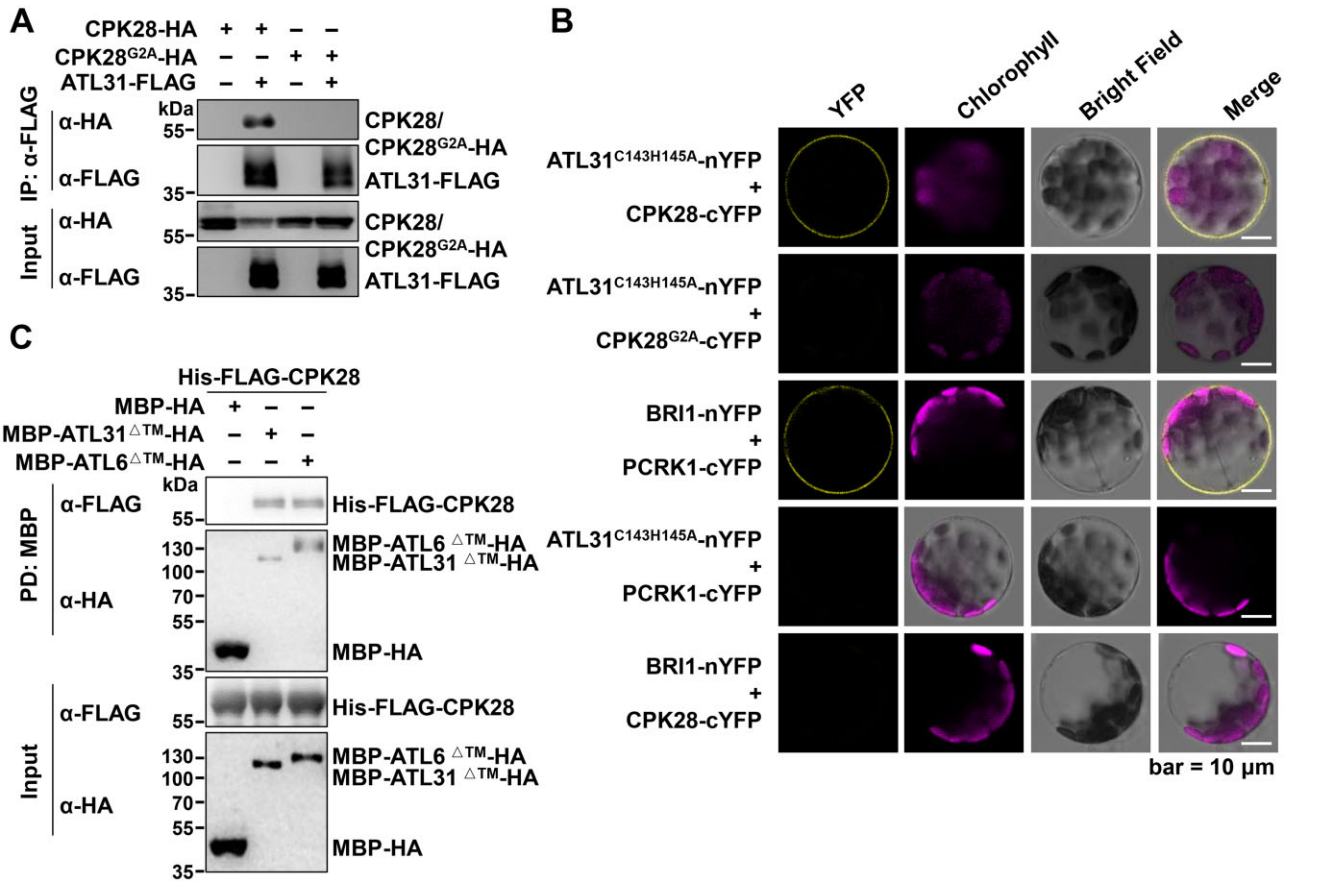

Figure 3 ATL31 interacts with CPK28 at the plasma membrane. A, ATL31 does not associate with CPK28^{G2A}. CPK28^{G2A}-HA and ATL31-FLAG were co-expressed in protoplasts. IPs were performed using anti-FLAG antibodies, and the associated proteins were detected by immunoblotting with anti-HA antibodies. B, ATL31^{C143H145A} associates with CPK28 at the plasma membrane. The indicated BiFC constructs were transfected into Arabidopsis protoplasts, and fluorescence was visualized by confocal microscopy. Scale bars, 10 μm. C, ATL31/6 directly interact with CPK28 *in vitro*. Recombinant MBP-HA, MBP-ATL31$^{\triangle TM}$-HA, or MBP-ATL6$^{\triangle TM}$ -HA proteins immobilized on amylose resin were incubated with His-FLAG-CPK28 proteins, and MBP PD assays were performed. △TM, lacking the transmembrane domain. Washed resin was subjected to immunoblotting with anti-HA and anti-FLAG antibodies to detect the immobilized proteins and the pulled-down proteins, respectively (top two parts). Input proteins were detected by immunoblotting with the indicated antibodies (bottom two parts).

ATL31^{C143H145A} variant exhibited much weaker autoubiquitination, suggesting that the ubiquitin ligase activity of ATL31^{C143H145A} is markedly weakened. Accordingly, ATL31^{C143H145A} was less effective than WT ATL31 at promoting CPK28 ubiquitination (Supplemental Figure S12).

To determine whether ATL31/6 directly ubiquitinate CPK28, we used a bacterial ubiquitination system that was previously developed in our laboratory (Han et al., 2017). ATL31/6-MYC, AtUBA1 (E1), AtUBC8 (E2), His- and FLAG-tagged ubiquitin (His-FLAG-Ub), and MBP-CPK28-HA were co-expressed in *Escherichia coli* BL21 strain. ATL31 and ATL6 exhibited autoubiquitination activity in this system, as detected with anti-MYC or anti-FLAG antibodies (Figure 4, B and C), which is consistent with previous reports (Sato et al., 2009; Maekawa et al., 2012). Both ATL31 and ATL6 directly ubiquitinated CPK28 in this bacterial system when UBC8 was used as the E2. The lack of E1, E2, ATL31/6, or ubiquitin resulted in the loss of CPK28 ubiquitination (Figure 4, B and C). Moreover, the mutation of C143 and H145 in ATL31 largely impaired its own ubiquitin ligase activity and resulted in decreased ubiquitination of CPK28 (Supplemental Figure S13A).

CPK28 interacts with BIK1 and promotes its turnover (Monaghan et al., 2014). However, ATL31 did not ubiquitinate either BIK1 or the cytosolic domain of BAK1 (BAK1CD; Supplemental Figure S13, B and C). Moreover, ATL2 did not ubiquitinate CPK28 (Figure 4D). These data further support the specificity of CPK28 ubiquitination by ATL31/6. Notably, we frequently observed some ubiquitination bands in the presence of E1, E2, and ubiquitin but not E3 during the detection of ubiquitin conjugates by immunoblotting with anti-FLAG antibodies (Figure 4, B–D; Supplemental Figure S13A). These ubiquitin conjugates were likely free ubiquitin chains generated by UBC8, as E2s such as UBC8, UBC7, UBC13, and UBC35 (with ubiquitin conjugating enzyme variant D together) could all generate free ubiquitin chains in the absence of E3, as previously shown (Zhao et al., 2013; Han et al., 2017; Turek et al., 2018).

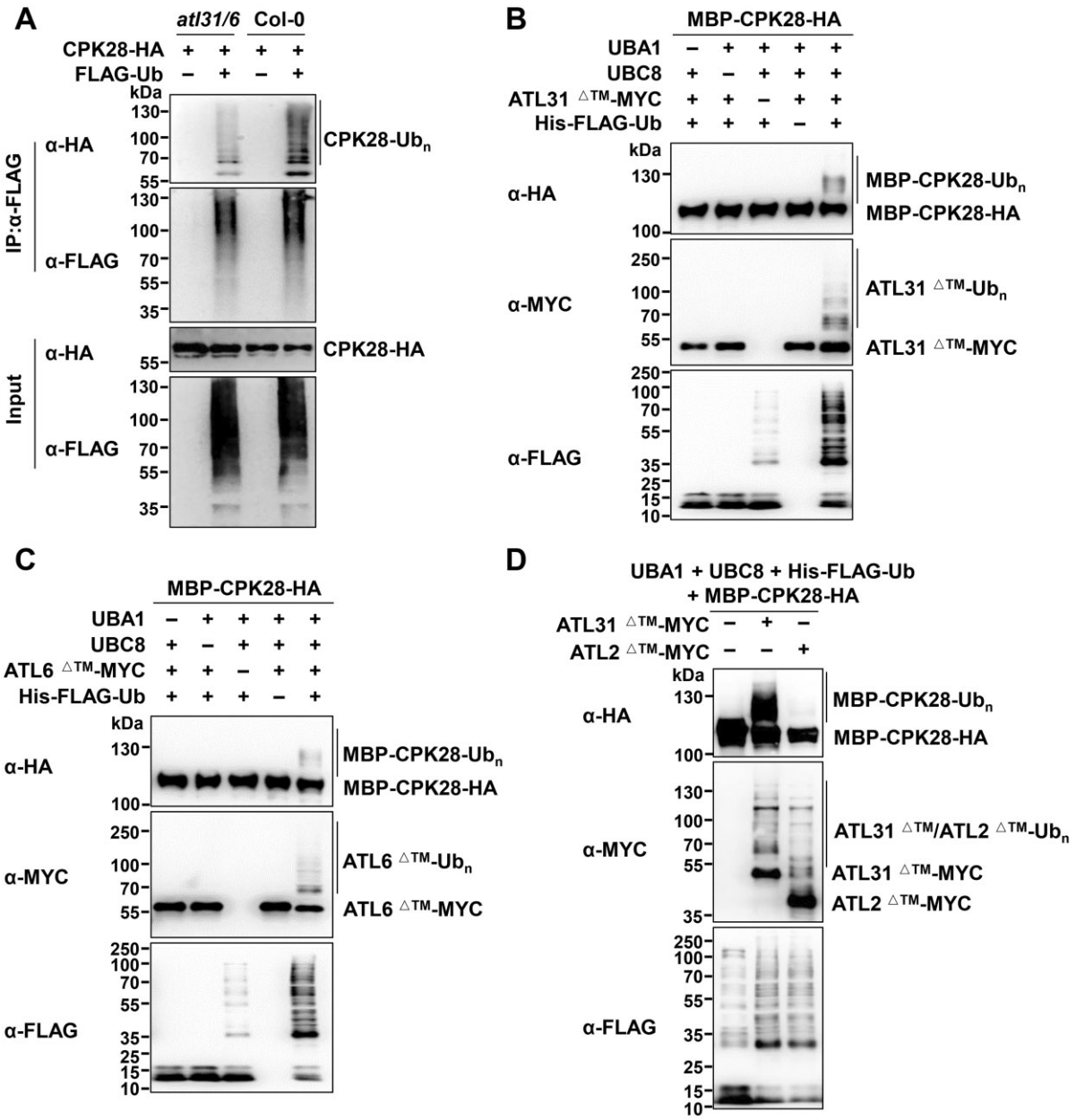

Figure 4 ATL31/6 ubiquitinate CPK28. A, CPK28 ubiquitination is weaker in *atl31 atl6* than in Col-0 plants. CPK28-HA and FLAG-Ub were co-expressed in protoplasts isolated from *atl31 atl6* or Col-0 plants. Following IP with anti-FLAG antibodies, the ubiquitination of CPK28 was detected by immunoblotting with anti-HA antibodies. B–D, ATL31/6 but not ATL2 directly ubiquitinate CPK28. The combination of ATL31$^{\triangle TM}$/ATL6$^{\triangle TM}$/ATL2$^{\triangle TM}$-MYC, AtUBA1 (E1), AtUBC8 (E2), His-FLAG-Ub, and MBP-CPK28-HA, or similar combinations lacking one component, were co-expressed in *E. coli*. The bacterial lysates were subjected to immunoblotting analysis with anti-HA antibodies to detect CPK28 ubiquitination, with anti-MYC antibodies to detect ATL31$^{\triangle TM}$/ATL6$^{\triangle TM}$/ATL2$^{\triangle TM}$ autoubiquitination, or with anti-FLAG antibodies to detect ubiquitin conjugates and free ubiquitin chains.

ATL31/6 mediate the proteasomal degradation of CPK28

We have shown that overexpressing *ATL31* in protoplasts significantly reduced CPK28-MYC protein abundance, but overexpressing *ATL41*, *ATL45*, and *ATL80* did not (Supplemental Figure S6). Like ATL31, its closest homolog ATL6 also mediated CPK28 degradation, but ATL2 did not, when they were co-expressed with CPK28-HA in Arabidopsis protoplasts (Supplemental Figure S14, A–C). PUB25 is known to interact with and serve as a substrate of CPK28 (Wang et al., 2018). Nonetheless, PUB25 did not affect CPK28 protein accumulation (Supplemental Figure S14D). Furthermore, ATL31/6 promoted CPK28 degradation in a dose-dependent manner (Figure 5, A and B). In contrast to WT ATL31, the ATL31^{C143H145A} variant was much less effective at promoting CPK28 protein degradation (Figure 5C). Although ATL31 mediated the degradation of WT CPK28, it barely contributed to the turnover of the CPK28^{G2A} variant (Figure 5D).

To further verify the role of ATL31/6 in mediating CPK28 degradation in plants, we monitored CPK28 protein

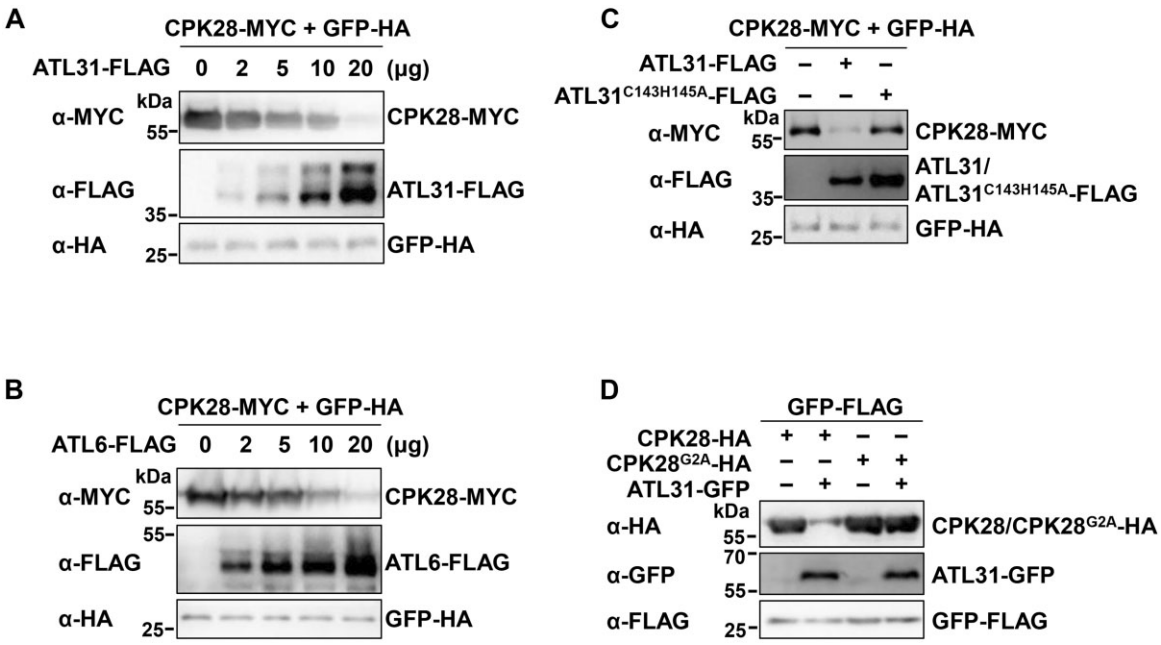

Figure 5 ATL31/6 promote the degradation of CPK28 in Arabidopsis protoplasts. A, B, ATL31/6 promote CPK28 degradation in a dose-dependent manner. Different amounts of ATL31- (A) or ATL6-FLAG (B) were co-expressed with CPK28-MYC in protoplasts. GFP-HA was used as an internal transfection control. CPK28-MYC/ATL31-FLAG/ATL6-FLAG/GFP-HA proteins were detected by immunoblotting with the indicated antibodies. C, ATL31^{C143H145A} is much less effective than ATL31 at promoting CPK28 protein degradation. ATL31- or ATL31^{C143H145A}-FLAG was co-expressed with CPK28-MYC in protoplasts. D, Overexpressing *ATL31* hardly reduces CPK28^{G2A} protein accumulation. ATL31-GFP was co-expressed with CPK28^{G2A}-HA or CPK28-HA in protoplasts. GFP-HA or GFP-FLAG was used as an internal transfection control (C and D).

accumulation in the *atl31 atl6* double mutant plants using anti-CPK28 antibodies. CPK28 protein levels were lower in Col-0 than in *atl31 atl6* (Supplemental Figure S15), while *CPK28* transcript levels in Col-0 were comparable to those in *atl31 atl6* plants (Supplemental Figure S16). Furthermore, in the presence of CHX, CPK28 degraded much more rapidly in Col-0 than in *atl31 atl6* plants, as measured with anti-CPK28 antibodies (Figure 6A). These results strongly support the notion that ATL31/6 mediate CPK28 degradation. Furthermore, in the presence of CHX, CPK28 protein levels decreased in Col-0 within 2 h of flg22 treatment (Figure 6B). However, this phenomenon did not occur in *atl31 atl6* plants (Figure 6B). These results suggest that ATL31/6 mediate flg22-enhanced CPK28 degradation. CPK28 directly phosphorylates BIK1 (Monaghan et al., 2014), and BIK1 was recently shown to transphosphorylate CPK28 (Bredow et al., 2021; Bredow and Monaghan, 2021). To test whether BIK1 affects CPK28 degradation, we measured CPK28 protein accumulation in *bik1* plants. CPK28 protein levels in *bik1* were comparable to those in Col-0 plants (Supplemental Figure S15).

We also performed cell-free degradation assays to confirm that ATL31/6 mediate the degradation of CPK28. In these assays, recombinant MBP-CPK28-HA was incubated with total protein extracts from Col-0 or *atl31 atl6* plants in the presence of ATP. The degradation rate of MBP-CPK28-HA was much slower in extracts from *atl31 atl6* than from Col-0. Moreover, when MG132 treatment was applied, the degradation of MBP-CPK28 was largely inhibited (Figure 6C). These results support the notion that ATL31/6 mediate CPK28 degradation in a 26S proteasome-dependent manner.

ATL31/6 modulate BIK1 homeostasis through CPK28

CPK28 is known to promote the degradation of BIK1 through PUB25/26 (Monaghan et al., 2014; Wang et al., 2018). We found that CPK28 accumulation was further regulated by ATL31/6. Therefore, we sought to determine whether ATL31/6 affect BIK1 accumulation. To this end, we transiently expressed *BIK1-HA* together with *ATL31/6-FLAG* in protoplasts. Overall, the accumulation of BIK1 was enhanced by *ATL31/6* overexpression, which slowed BIK1 turnover (Figure 7, A and B; Supplemental Figure S17A), likely due to the degradation of CPK28 mediated by ATL31/6 (Figure 6). In contrast, overexpressing *ATL31*^{C143H145A} or *ATL2* in protoplasts had little effect on BIK1 accumulation (Supplemental Figure S17, A and B), and overexpressing *ATL31* barely affected the accumulation of FLS2 and BAK1 (Supplemental Figure S17, C and D). Furthermore, when BIK1-HA was transiently expressed in protoplasts isolated from *alt31 atl6* and Col-0, overall BIK1-HA protein levels were lower in *alt31 atl6* than in Col-0, and BIK1 turnover was accelerated in *alt31 atl6* compared to that in Col-0 (Figure 7C). These results suggest that ATL31/6 promote BIK1 protein accumulation.

To confirm that ATL31/6 modulate the stability of BIK1 via CPK28, we examined the effect of *ATL31* overexpression on BIK1 accumulation in the *cpk28* mutant (Monaghan et al., 2014). BIK1-HA protein levels were higher in *cpk28* protoplasts than in Col-0, which is consistent with previous reports (Monaghan et al., 2014; Wang et al., 2018). When BIK1 was co-expressed with ATL31, BIK1 protein

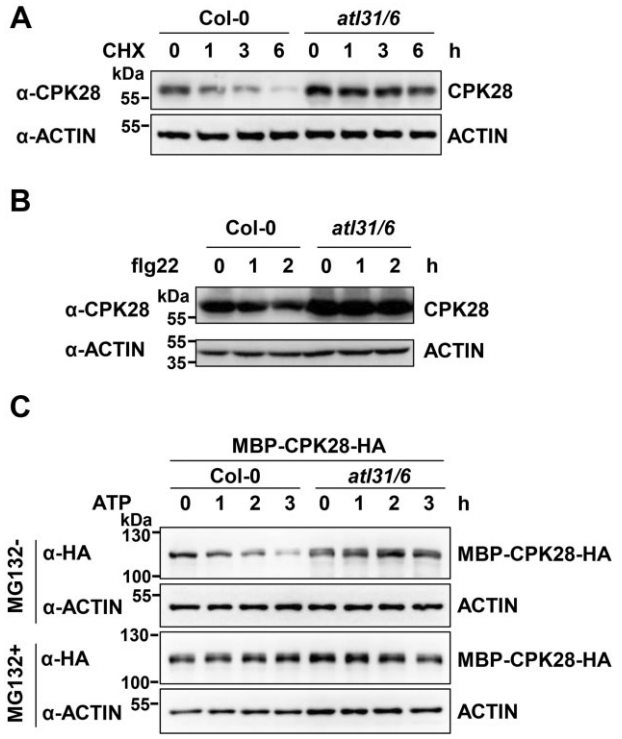

Figure 6 The degradation of CPK28 in *atl31 atl6* and Col-0 plants. A, CPK28 protein turnover in *atl31 atl6* and Col-0 plants. Seven-day-old Col-0 and *atl31 atl6* seedlings (10 seedlings per sample) were treated with 100-μM CHX for different times. B, flg22-induced CPK28 degradation is largely blocked by loss of *ATL31/6* function. Seven-day-old Col-0 and *atl31 atl6* seedlings (10 seedlings per sample) were pretreated with 100-μM CHX, followed 1 h later by treatment with 2-μM flg22 for the indicated times. A, B, Total proteins were isolated from whole seedlings. CPK28 proteins were detected by immunoblotting with anti-CPK28 antibodies. ACTIN was used as a loading control. C, ATL31/6 mediate the proteasomal degradation of CPK28, as demonstrated by cell-free degradation assays. Purified recombinant MBP-CPK28-HA proteins were incubated with total protein extracts isolated from 14-day-old Col-0 or *atl31 atl6* seedlings in the presence of 1-mM ATP for the indicated times, with or without 50-μM MG132. MBP-CPK28-HA was detected with anti-HA antibodies. ACTIN was detected as a loading control.

accumulation in Col-0 protoplasts was enhanced to a level comparable to that in *cpk28* protoplasts. However, ATL31 had little effect on promoting BIK1 protein accumulation in *cpk28* protoplasts (Figure 7D). These results demonstrate that ATL31 modulates BIK1 homeostasis through CPK28.

ATL31/6 positively regulate BIK1-mediated immunity

BIK1 plays a critical role in flg22-triggered production of ROS (Kadota et al., 2014; Li et al., 2014), and *cpk28* mutant plants produce more ROS than Col-0 plants upon flg22 treatment (Monaghan et al., 2014). We therefore tested whether *ATL31/6* regulate the flg22-triggered ROS burst. After flg22 treatment, the *atl31 and atl6* single mutants exhibited less ROS production than Col-0 plants, and the *atl31 atl6* double mutant plants produced even less ROS than either single mutant (Figure 8A), suggesting that ATL31 and ATL6 play redundant roles in positively regulating PTI signaling.

flg22 also triggers MITOGEN-ACTIVATED PROTEIN KINASE (MAPK) activation (Segonzac et al., 2014, Xu et al., 2014). flg22-induced MPK3/6 activation was not affected by the loss of *ATL31 and ATL6* (Figure 8B), which is in line with a previous observation that overexpression of *CPK28* had no impact on MPK3/6 activation (Monaghan et al., 2014).

As BIK1 plays an important role in stomatal immunity (Li et al., 2014; Thor et al., 2020), we also measured flg22-induced stomatal closure in Col-0 and *atl31 atl6* plants. As observed in the immune-deficient mutant *bik1* (Li et al., 2014) and in transgenic plants overexpressing *CPK28* (Monaghan et al., 2014), flg22-induced stomatal closure was almost abolished in *atl31 atl6* mutant plants compared to that in Col-0 (Figure 8C). However, abscisic acid (ABA)-triggered stomatal closure was not affected in *atl31 atl6* (Figure 8D), suggesting that ATL31/6 specifically function in stomatal closure during innate immunity. Moreover, *atl31 atl6* plants were more susceptible than Col-0 to the hypovirulent bacterial pathogen *Pseudomonas syringae* pv. *tomato* (*Pst*) DC3000 *COR*$^-$, a strain deficient in the production of the phytotoxin coronatine (COR), which stimulates stomatal opening (Ma et al., 1991; Melotto et al., 2006; Figure 8E). We also inoculated *atl31 atl6*, *cpk28-1*, and Col-0 plants with the nonvirulent type III secretion mutant strain *Pst* DC3000 *hrcC*$^-$. *atl31 atl6* also supported significantly higher bacterial growth than Col-0 plants, whereas the *cpk28* mutant exhibited stronger resistance to bacteria than Col-0 (Supplemental Figure S18), which is consistent with a previous report (Monaghan et al., 2014). These results demonstrate that ATL31/6 positively regulate BIK1-mediated immunity.

Discussion

Immune responses must be tightly regulated to ensure their proper timing, appropriate amplitude, and optimal duration. BIK1 functions as a signaling hub of plant immunity and is subjected to different modes of modification, including phosphorylation and poly- and monoubiquitination (Lu et al., 2010; Zhang et al., 2010; Monaghan et al., 2014; Wang et al., 2018; Ma et al., 2020). Importantly, an immune signaling module forms to modulate BIK1 stability and immune homeostasis in which CPK28 phosphorylates PUB25/26 to enhance their activity, thereby promoting BIK1 degradation (Monaghan et al., 2014; Wang et al., 2018). Here, we demonstrated that CPK28 is further subjected to negative regulation by ATL31/6. Our findings indicate that the PRR–BIK1 immune complex is subjected to multi-layered regulation, and CPK28 is kept in check to maintain BIK1 homeostasis. Furthermore, we demonstrate how ATL31/6-mediated CPK28 degradation is dynamically controlled to regulate immune singling. In the resting state, ATL31/6 regulate CPK28 turnover to maintain immune homeostasis. Following flg22 treatment, the degradation of CPK28 was enhanced, which resulted in the relief of the CPK28-mediated negative

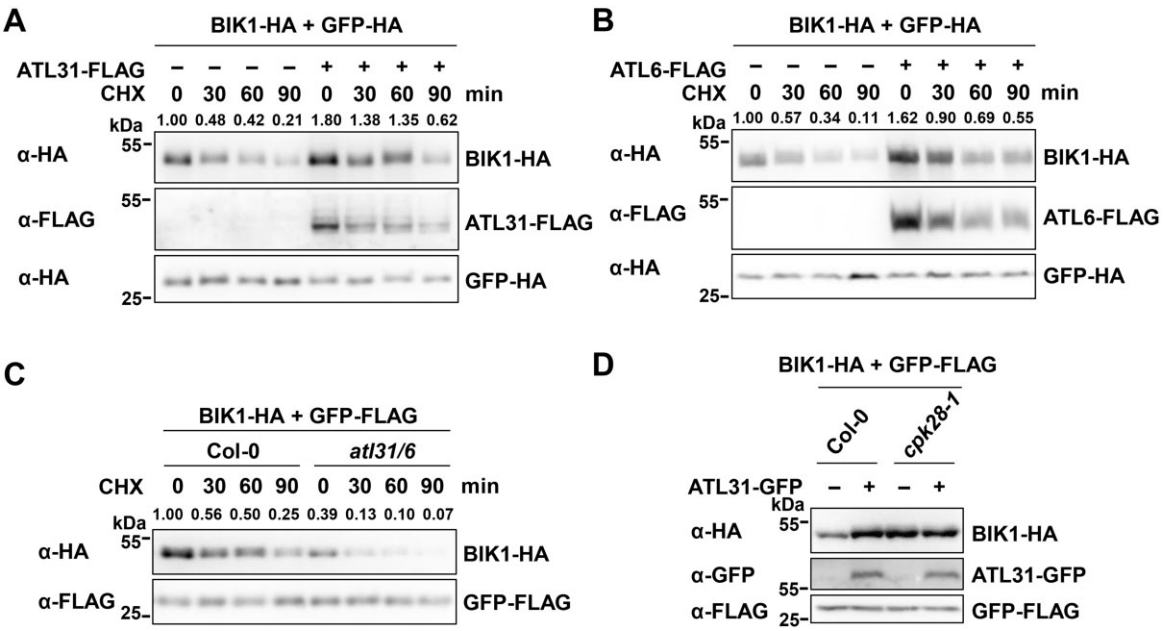

Figure 7 ATL31/6 modulate BIK1 homeostasis. A, B, ATL31/6 promote BIK1 accumulation. BIK1-HA was co-expressed with ATL31/6-FLAG in protoplasts. The protoplasts were treated with 50-μM CHX for the indicated times before harvesting. BIK1-HA proteins were detected by immunoblotting with anti-HA antibodies. GFP-HA was used as an internal transfection control. The relative protein levels of BIK1-HA were normalized to those of GFP-HA. The relative protein level of BIK1-HA at the beginning of the CHX treatment (in the absence of ATL31-FLAG) was set to 1. The density of the BIK1-HA and GFP-HA protein bands was quantified using EvolutionCapt v18.10 software. C, BIK1-HA protein levels are lower in *atl31 atl6* than in Col-0 protoplasts. BIK1-HA was expressed in protoplasts isolated from *atl31 atl6* or Col-0 plants. The protoplasts were treated with 50-μM CHX for the indicated times. GFP-FLAG was used as an internal transfection control. The relative protein levels of BIK1-HA were normalized to those of GFP-FLAG. The relative protein level of BIK1-HA in Col-0 at the beginning of the CHX treatment was set to 1. D, ATL31 modulates BIK1 homeostasis via CPK28. BIK1-HA was co-expressed together with or without ATL31-GFP in protoplasts isolated from Col-0 or *cpk28-1* plants. GFP-FLAG was used as an internal transfection control. BIK1-HA proteins were detected by immunoblotting with anti-HA antibodies.

regulation of the immune receptor complex to further enhance immune responses (Figure 9). It was recently reported that *CPK28* transcripts are alternatively spliced after flg22 (Bazin et al., 2020) and AtPep1 treatment (Dressano et al., 2020), resulting in the accumulation of the truncated *CPK28* variants, which has been proposed as a major immune-induced CPK28 attenuation mechanism. Therefore, flg22-induced CPK28 degradation has emerged as another CPK28 attenuation mechanism. Notably, the canonically spliced *CPK28* transcript was also induced upon flg22 treatment; however, its induction was weaker and slower than that of *CPK28*-RI (Supplemental Figure S8). Therefore, it is likely that the induction of WT *CPK28* by flg22 acts as a negative feedback regulation to maintain immune homeostasis. On the other hand, this result indicates that the negative immune regulator genes can also be induced by PAMP treatment, like *PUB22*, *PUB23*, and *PUB24* (Trujillo et al., 2008).

The ubiquitination and proteasomal degradation of positive regulators of plant immunity has often been shown to contribute to their degradation and the attenuation of immune signaling, except for the monoubiquitination of BIK1 by RHA3A and RHA3B (Stegmann et al., 2012; Monaghan et al., 2014; Lee et al., 2020; Wang et al., 2018; Ma et al., 2020). In contrast, less is known about the ubiquitination and proteasomal degradation of negative immune regulators, which may contribute to activation of immune signaling. Here, we showed that negative immune regulators such as CPK28, BIR2, and BIR3 also undergo ubiquitination and proteasomal degradation (Figure 1B; Supplemental Figure S1, A and B). In line with this, a recent proteomics study identified ubiquitination sites on CPK28, BIR2, and BIR3 proteins (Grubb et al., 2021). We showed that CPK28 was ubiquitinated by ATL31/6, leading to its degradation. However, which E3 ligases mediate the ubiquitination and degradation of BIR2 or BIR3 should be investigated in the near future.

ATL is a RING-type ubiquitin ligase gene family unique to plants that consists of 91 members in Arabidopsis (Aguilar-Hernández et al., 2011; Guzmán, 2014). Several ATL family members are involved in defense response. Ectopic expression of *ATL2* leads to the induction of many defense-related genes (Serrano and Guzman, 2004). Here, we demonstrated that ATL2 does not associate with and ubiquitinate CPK28 (Figure 2, G and D); consequently, it does not mediate CPK28 degradation (Supplemental Figure S14C). Moreover, ATL9, another ATL family member that is localized to the endoplasmic reticulum, positively regulates plant resistance to the biotrophic fungal pathogen *Golovinomyces cichoracearum* (Berrocal-Lobo et al., 2010). Although ATL31 and ATL6 positively regulate plant resistance to *Pst* DC3000 infection (Maekawa et al., 2012), the underlying mechanism remains elusive. Here, by screening for ubiquitin ligases that mediate CPK28 degradation, we identified ATL31 and ATL6

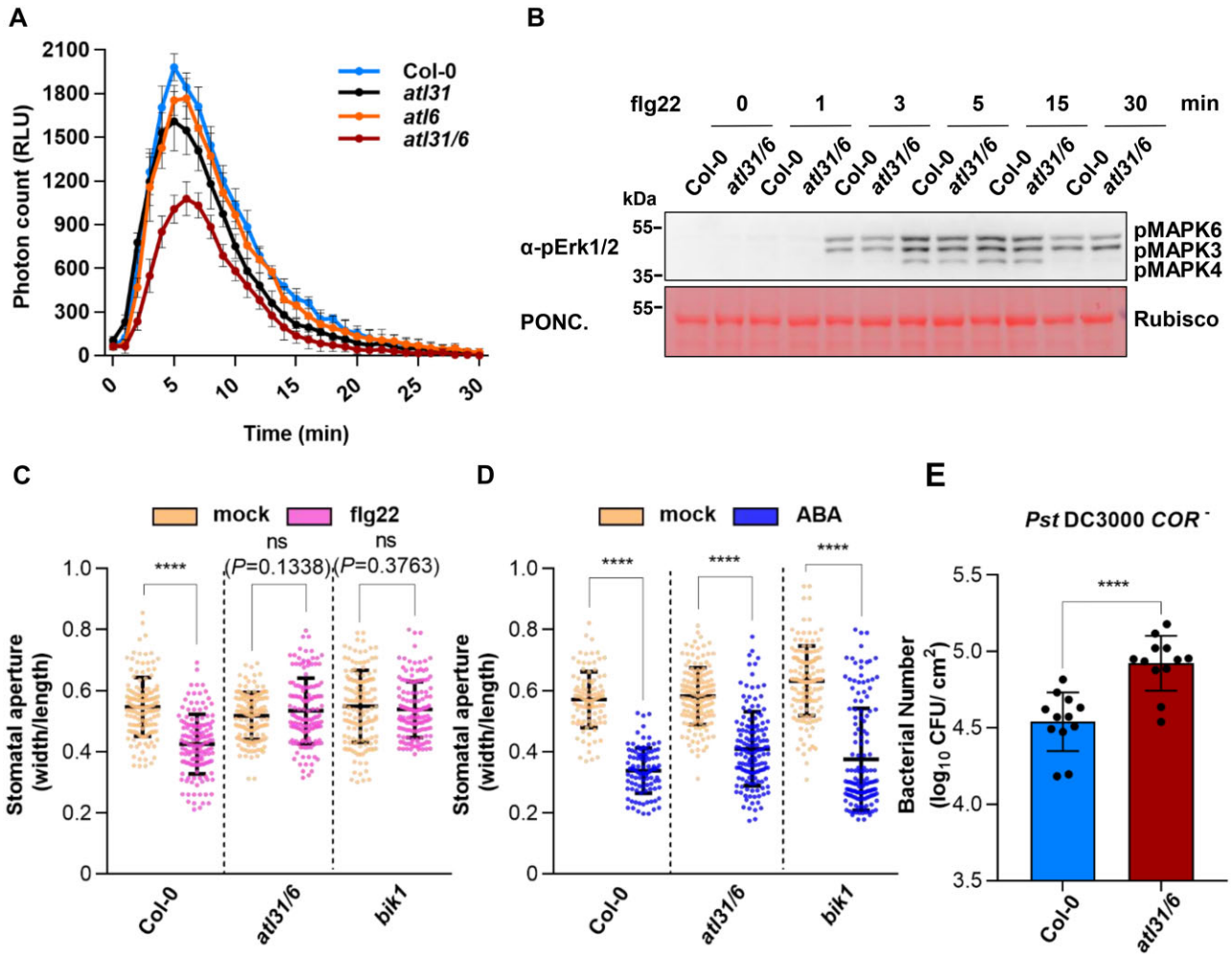

Figure 8 *ATL31/6* positively regulate BIK1-mediated immunity. A, *atl31*, *atl6*, and *atl31 atl6* produce less ROS than Col-0 after flg22 treatment. Leaf discs from 30-day-old plants of the indicated genotypes were treated with 100-nM flg22, and RLU (representing the relative amounts of H_2O_2) were immediately measured. Values are means ± SD (n = 8, n means leaf disc number). B, flg22-induced MPK3/6 activation in *atl31 atl6* and Col-0 plants. Seven-day-old seedlings (10 seedlings per sample) were treated with 100-nM flg22 for the indicated times. Total proteins were isolated from whole seedlings. MAPK activation was detected by immunoblotting with anti-pErk1/2 antibodies. Ponceau (PONC.) staining of the membrane was used as the loading control. C, flg22-triggered stomatal closure in *atl31 atl6* and Col-0 plants. Leaves from 5-week-old Col-0, *atl31 atl6*, and *bik1* plants were treated with 10-μM flg22 for 1 h. The stomatal aperture was measured using ImageJ software. Each data point represents a single stoma; values are means ± SD for n = 144 stomata from three biological repeats using independent plant samples grown and treated with flg22 under the same conditions. D, ABA-triggered stomatal closure in *atl31 atl6* and Col-0 plants. Leaves from 5-week-old Col-0, *atl31 atl6*, and *bik1* plants were treated with 10-μM ABA for 1 h. The stomatal aperture was measured using ImageJ software. Each data point represents a single stoma; values are means ± SD for n > 100 stomata from three biological repeats using independent plant samples grown and treated with ABA under the same conditions. C, D, Statistical significance compared to mock-treated plants was determined by Student's t tests: ****P < 0.0001; ns, no significant difference. Number of stomata counted and statistical analysis are described in detail in the "Materials and methods" and Supplemental Table S3. E, Growth of *Pst* DC3000 *COR*$^-$ in Col-0 and *atl31 atl6* plants. Four-week-old Col-0 and *atl31 atl6* plants were dipping-inoculated with the bacteria. Bacterial growth was evaluated as colony-forming units per cm^2 of leaf area (cfu/cm^2) and was determined 3 days post inoculation. Individual data points are shown with means ± SD (n = 12 leaves from three biological replicates using plant samples grown and inoculated under the same conditions). Statistical significance compared to Col-0 plants was determined by Student's t tests: ****P < 0.0001 (Supplemental Table S3).

as the cognate E3s that target CPK28 for ubiquitination and proteasomal degradation. However, the substrates of ATL2 and ATL9 have yet to be identified and warrant further investigation.

The E3 ligases ATL44 and ATL45, also known as RHA3A and RHA3B, respectively, were recently shown to play positive roles in activating immune signaling by mediating the monoubiquitination of BIK1, resulting in the release of BIK1 from the FLS2 PRR complex (Ma et al., 2020). Therefore, ATL-mediated protein ubiquitination not only has proteolytic functions, but also plays a nonproteolytic role in regulating immune responses.

Ub chains with different linkage types encode different signals that dictate the fates of their modified substrates. The

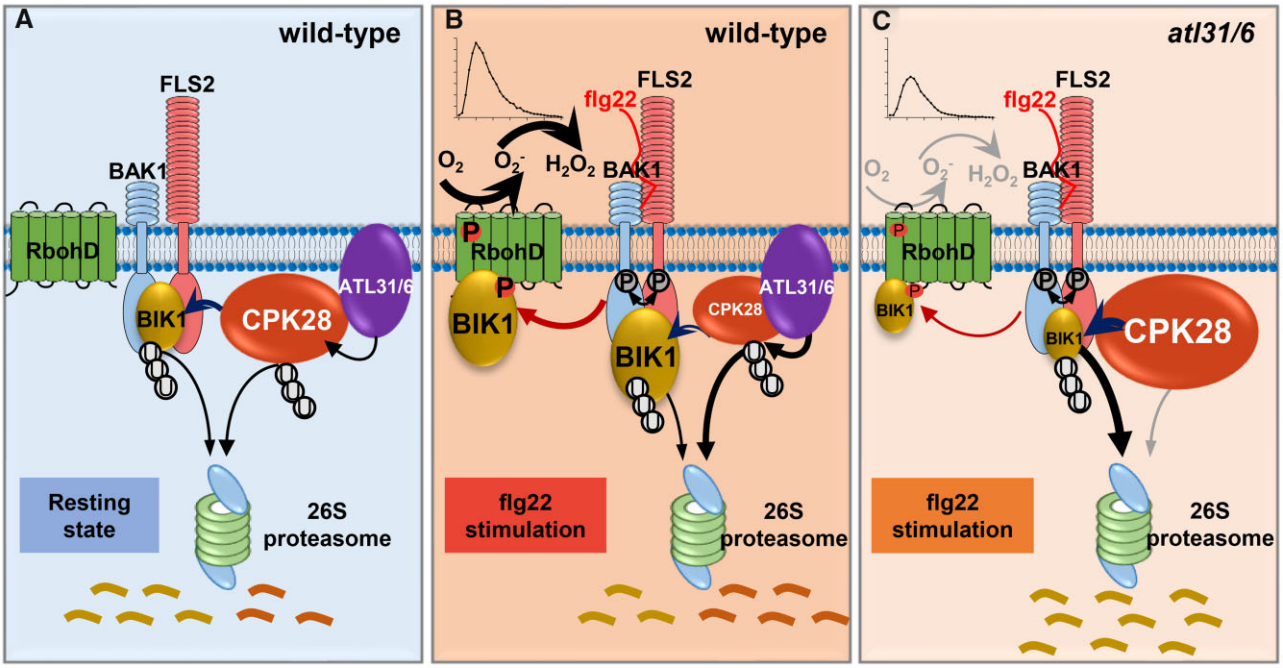

Figure 9 CPK28 is targeted by ATL31 and ATL6 for proteasome-mediated degradation to fine-tune immune signaling. BIK1 acts as a signaling hub of plant immunity, which relays the immune signal from the FLS2-BAK1 complex to RbohD to promote ROS production. BIK1 homeostasis is maintained by a regulatory module in which CPK28 contributes to BIK1 turnover. Based on a previous conceptual model (Monaghan et al., 2014), we proposed a model for maintenance of BIK1 homeostasis by ATL31/6 via CPK28. Our work demonstrates that CPK28 is under proteasomal control to fine-tune immune signaling. The ubiquitin ligases ATL31 and ATL6 interact with CPK28 at the plasma membrane. ATL31/6 directly ubiquitinate CPK28, which results in the degradation of CPK28 via the 26S proteasome. A, In the resting state, ATL31/6 mediate CPK28 turnover to maintain BIK1 homeostasis. B, Following flg22 treatment, the association of CPK28 and ATL31/6 is enhanced, which promotes the degradation of CPK28 and leads to the relief of the CPK28-mediated negative regulation of the immune receptor complex to enhance immune responses. C, CPK28 protein accumulation is higher in *atl31 atl6* than in Col-0. Consequently, BIK1 protein levels are lower in *atl31 atl6* than in Col-0. Therefore, the immune responses in *atl31 atl6* are reduced compared to those of Col-0.

Lys48 Ub chain usually encodes a signal for 26S proteasomal degradation, while Lys63 Ub chains often play nonproteolytic roles (Komander and Rape 2012). E2s play a critical role in ubiquitin chain assembly (Komander and Rape 2012; Stewart et al., 2016). The Arabidopsis genome encodes 37 E2 enzymes. UBC8 is one of the Group VI E2s that consist almost exclusively of the UBC domain that binds to E3s (Kraft et al., 2005; Turek et al., 2018). We previously showed that UBC8 had broad lysine specificity, and likely mediated the formation of Ub chains at both the Lys48 and Lys63 sites or at other Lys sites of Ub moieties (Han et al., 2017). UBC8, as well as other group VI E2 members, functions with a wide range of E3 ubiquitin ligases (Kraft et al., 2005). Therefore, UBC8 is widely used for *in vitro* ubiquitination assays to examine the ubiquitination of various substrates by cognate E3s (Lu et al., 2011; Stegmann et al., 2012; Wang et al., 2018; Ma et al., 2020). A set of E2s that paired with PUB22 *in vivo* were recently identified, including various members of group VI, such as UBC8 and UBC30 (Turek et al., 2018). Here, we also used UBC8 as the E2 and demonstrated the ubiquitination of CPK28 by ATL31/6 (Figure 4, B–D). However, to uncover the type of CPK28 ubiquitination mediated by ATL31/6 and to fully understand the distinct cellular roles played by ATL31/6, an endogenous E2 for ATL31/6 needs to be identified.

C and N in plants function not only as energy sources but also as signaling molecules. C and N are reciprocally regulated and tightly integrated to maintain their proper balance. The ratio of C and N (C/N) is sensed in plant cells, and C/N-nutrient responses are initiated to regulate plant growth and development (Vidal and Gutierrez, 2008). ATL31/6 negatively regulate plant C/N responses via the ubiquitination and subsequent degradation of 14-3-3 proteins (Sato et al., 2009, 2011). In this study, we showed that ATL31/6 function as positive regulators of plant immune responses by mediating CPK28 ubiquitination. C and N metabolism is thought to be related to plant defense responses (Gómez-Ariza et al., 2007; Ros et al., 2008; Maekawa et al., 2012). Therefore, it is likely that ATL31/6 function in the crosstalk between plant immune signaling and C/N responses, but this requires further investigation. Additionally, whether CPK28 is involved in regulating plant C/N responses remains to be determined.

Our results demonstrate that ATL31/6 target CPK28 for ubiquitination and degradation. A previous study revealed that eight 14-3-3 isoforms are associated with ATL31. Of these 14-3-3s, 14-3-3χ and 14-3-3λ directly interact with ATL31 (Sato et al., 2011). Furthermore, 14-3-3χ serves as a substrate of ATL31 and thus is ubiquitinated and targeted for 26S proteasome-mediated degradation in response to

cellular C/N changes (Sato et al., 2011). 14-3-3 proteins bind to the specific phosphorylated motifs in a wide array of target proteins and play important roles in various cellular processes, including plant defense responses (Roberts et al., 2002; Chevalier et al., 2009). 14-3-3 proteins play positive roles in regulating early PTI responses in Arabidopsis, such as PAMP-triggered ROS burst and stomatal immunity, as chemical disruption of the interaction between 14-3-3s and their client proteins greatly suppressed these immune responses (Lozano-Durán et al., 2014). In addition, 14-3-3λ binds to RPW8.2 (RESISTANCE TO POWDERY MILDEW8.2) and positively regulates RPW8.2-mediated resistance to the fungal pathogens *Golovinomyces* spp. in Arabidopsis via the salicylic acid signaling pathway (Yang et al., 2009). Notably, CPK28 and other CPKs phosphorylated 14-3-3χ and 14-3-3ε *in vitro* kinase assays. Furthermore, CPK28 harbors a canonical 14-3-3 binding motif R-S/T-X-S^{43}-X-P; and Ser43 in this motif is an autophosphorylation site of CPK28 (Swatek et al., 2014). However, whether these 14-3-3 isoforms are involved in ATL31-mediated CPK28 degradation and in regulating CPK28-mediated immunity remain to be determined.

CPK28 plays dual roles in regulating immune signaling and stem elongation (Matschi et al., 2013, 2015). After the induction of bolting, *cpk28* mutant plants displayed reduced stem elongation compared to the WT plants (Matschi et al., 2013, 2015). Like *CPK28* overexpression lines (Monaghan et al., 2014), *atl31 atl6* plants did not show a growth defect after the transition to the reproductive stage (Supplemental Figure S11G). However, whether ATL31/6 regulate stem elongation and whether they mediate CPK28 degradation in a stage-specific manner remain to be investigated.

The phosphorylation status of a kinase affects its ubiquitination by cognate E3 ligases. BIK1 phosphorylation is a prerequisite for its monoubiquitination at the plasma membrane (Ma et al., 2020). In contrast, flg22-induced phosphorylation at Ser236/Thr237 of BIK1 inhibits its polyubiquitination by PUB25/26 (Wang et al., 2018). CPK28 undergoes autophosphorylation at multiple sites (Hegeman et al., 2006; Matschi et al., 2013; Swatek et al., 2014; Bender et al., 2017). The kinase activity of CPK28 is required for its roles in stem elongation and immune homeostasis (Matschi et al., 2013; Monaghan et al., 2014). flg22 treatment can promote CPK28 kinase activity (Wang et al., 2018). However, the sites undergoing flg22-induced phosphorylation have not been identified for CPK28. CPK28 was recently shown to undergo intermolecular autophosphorylation at Ser318, which can also be transphosphorylated by BIK1 (Bredow et al., 2021). Moreover, phosphorylation of Ser318 is required for CPK28 activation at physiological [Ca^{2+}] and CPK28-mediated immune homeostasis, but not required for stem elongation (Bredow et al., 2021). Additionally, Thr76 of CPK28, a conserved BIK1 phosphorylation site but not an autophosphorylation site, is also required for CPK28-mediated immune regulation (Bredow and Monaghan, 2021). It would be interesting to examine whether the autophosphorylation of CPK28 and the phosphorylation of CPK28 at Ser318/Thr76 are required for its ubiquitination by ATL31/6 and subsequent proteosomal degradation. We observed that CPK28 protein levels in *bik1* plants were comparable to those of Col-0 plants (Supplemental Figure S15). It is likely that phosphorylation of CPK28 by BIK1 does not affect CPK28 protein accumulation. However, BIK1 and its closest homolog PBL1 function additively in PTI signaling (Zhang et al., 2010). To investigate the role of BIK1 in CPK28 accumulation, it is necessary to use the *bik1 pbl1* double mutant, as a recent epistasis analysis demonstrates CPK28-mediated immune signaling is dependent on both BIK1 and PBL1 (Bredow et al., 2021). Intriguingly, CPK28-RI has been shown to have impaired kinase activity and compromised autophosphorylation (Dressano et al., 2020), but whether CPK28-RI is ubiquitinated by ATL31/6 and undergoes degradation await more investigation.

Materials and methods

Plant materials and growth conditions

For protoplast isolation, the stomatal aperture assay, and the pathogen infection assay, *A. thaliana* plants were grown in soil (TS 1, Lithuania) in a growth room at 22°C with a 60% relative humidity and under 70 μE m^{-2} s^{-1} light (white fluorescent bulbs) with a 12-h photoperiod for 30 days. For assays using Arabidopsis seedlings, seeds were surface sterilized, germinated and grown on 1/2 Murashige and Skoog plates with 0.5% sucrose and 0.8% agar. The plates were kept in the dark at 4°C for 2 days, and then the plants were grown under the same conditions described above. The *fls2*, *bak1-4*, and *bik1* mutants were described previously (Shan et al., 2008; Lu et al., 2010). The T-DNA insertion mutants *atl31* (GK_746D08, Sato et al., 2009), *atl6* (Salk_149614, Sato et al., 2009), *cpk28-1* (WiscDslox246D03, Monaghan et al., 2014), and *cpk28-3* (GABI_523B08, Monaghan et al., 2014) were obtained from the Arabidopsis Biological Resource Center (ABRC), genotyped by PCR-based methods, and confirmed by RT-PCR analysis. The *atl31 atl6* double mutant was generated through a genetic cross between *atl31* and *atl6* (Sato et al., 2009, 2011) and confirmed by molecular genotyping and RT-PCR analysis. The primers used for genotyping are listed in Supplemental Table S2.

Elicitors and antibodies

The flg22 peptide (QRLSTGSRINSAKDDAAGLQIA) was synthesized by the Shanghai Biotech Company (Shanghai, China).

Anti-CPK28 antibodies were generated in mouse by the Animal Facility, Institute of Genetics and Developmental Biology (Beijing), using full-length recombinant CPK28 proteins as antigens. The rabbit polyclonal anti-Phospho-p44/42 MAPK (Erk1/2) antibody (Cat# 9101) was purchased from Cell Signaling Technology (USA). The anti-HA antibody (Cat# H3663), mouse monoclonal anti-FLAG antibody (Cat# F1804), mouse monoclonal anti-HA-peroxidase (Cat# H6533), mouse monoclonal anti-FLAG-peroxidase (Cat# A8592), and mouse monoclonal anti-C-MYC-peroxidase (Cat# A5598) were purchased from Sigma (USA). The goat

polyclonal anti-GFP-peroxidase (Cat# ab6663) was purchased from Abcam (USA). The mouse monoclonal anti-plant beta-ACTIN antibody (Cat# AT0004) was purchased from CMCTAG (USA) and used at 1:10,000 dilution. The goat anti-rabbit & mouse IgG-HRP (Cat#M21003-S) was purchased from Abmart (China) and used at 1:10,000 dilution.

Plasmid construction

The full-length coding sequences of Arabidopsis *CPK28*, *CPK8*, *CPK6*, *CPK1*, *CPK3*, *CPK16*, *CPK28*-RI, *BIR2*, *BIR3*, *ATL31*, *ATL6*, *ATL2*, *PUB25*, *PBL13*, *RCN1* and a set of E3 ubiquitin ligase genes were amplified by PCR from Col-0 cDNA and cloned into the plant expression vector pHBT, where they were fused to either an HA, FLAG, MYC, cYFP, nYFP, GFP, or RFP tag.

Arabidopsis *FLS2*, *BAK1*, *BIK1*, *UBQ10*, *BRI1*, *PCRK1*, and *GFP* constructs were described previously (Huang et al., 2019; Lu et al., 2010, 2011). *CPK28*, *CPK8*, *CPK6*, *CPK1*, *CPK3*, *CPK16*, *CPK28*-RI, *ATL31*$^{\triangle TM}$ (amino acids 67–368), and *ATL6*$^{\triangle TM}$ (amino acids 71–398) were subcloned into the modified His-tagged or MBP-tagged fusion protein expression vector pET28a (Novagen) or pMAL-C2 (New England Biolabs). The primers used are listed in Supplemental Table S2.

RT-qPCR

Total RNA was extracted from 7-day-old seedlings using TRIzol (Invitrogen) following the manufacturer's instructions. The first-strand cDNA was synthesized in 20-μL reactions from 1 μg DNase I-treated total RNA using a reverse transcription kit (Promega, USA). qPCR was then performed on a Bio-Rad CFX-96 Real-Time PCR system using a SYBR Green qPCR kit (Promega, USA). Gene expression levels were normalized to that of *GAPC*, a stably expressed reference gene (Czechowski et al., 2005).

Transcriptome sequencing

Seven-day-old Arabidopsis seedlings were treated with 4-μM flg22 or water for 30 min. Total RNA was isolated from the seedlings using TRIzol reagent (Invitrogen). Library construction and sequencing were performed by Novogene (Tianjing, China). In-house Perl scripts were used to process the raw reads, and the clean data were obtained by calculating Q20, Q30, and GC content. The clean reads were aligned to the reference Arabidopsis genome using TopHat v2.0.12. The number of fragments per kilobase of transcript sequence per million base pairs sequenced was counted using HTSeq v0.6.1 (Trapnell et al., 2009). Differential expression analysis of seedlings treated with flg22 or water for two biological replicates (independent seedling samples grown and treated with flg22 or water under the same conditions) was performed using the DESeq R package (1.18.0). A model based on the negative binomial distribution was used to calculate *P*-values for differential expression, which were further adjusted using the Benjamini and Hochberg approach. Differentially expressed genes were defined as those with $P < 0.05$.

Transient gene expression in protoplasts

Arabidopsis leaf protoplasts were isolated and used for transient gene expression as described previously (Huang et al., 2019). Protein expression in protoplasts was then detected by immunoblotting with anti-HA, anti-FLAG, anti-MYC, or anti-GFP antibodies.

Co-IP assays

Co-IP assays were performed as described by Huang et al. (2019). Protoplasts were transfected and incubated for 10 h. Before being harvested, the protoplasts were treated with 2-μM flg22 or water for 30 min. Total proteins were extracted from the protoplasts with protein extraction buffer containing 1-mM EDTA, 0.5% Triton X-100 and a protease inhibitor cocktail tablet (Roche). After centrifugation (12,470*g*) at 4°C for 10 min, the supernatant was incubated with anti-FLAG antibodies (Sigma) at 4°C for 2 h and then protein-G-agarose beads (Roche) were added and the incubation was continued for another 2 h. The agarose beads were collected by centrifugation (100*g*) at room temperature for 2 min, washed three times with washing buffer containing 1-mM EDTA and 0.1% Triton X-100, and washed once with 50-mM Tris–HCl at pH 7.5. The immunoprecipitated proteins were detected by immunoblotting.

BiFC assay in Arabidopsis protoplasts and confocal laser-scanning microscopy

Arabidopsis protoplasts were transfected with the BiFC vectors *ATL31C*^{143H145A}*-nYFP*, *CPK28-cYFP*, *CPK28*^{G2A}*-cYFP*, *BRI1-nYFP*, and *PCRK1-cYFP*. Fluorescent signals were detected by confocal laser-scanning microscopy (Leica, Germany). YFP was excited at 514 nm using an argon laser, and emission was collected from 525 to 570 nm. GFP was excited at 488 nm using an argon laser, and emission was collected at 500–540 nm. RFP was excited at 552 nm using an argon laser, and emission was collected between 589 and 625 nm. The chlorophyll autofluorescence was collected at wavelengths between 630 and 700 nm.

Recombinant protein expression, purification, and MBP PD assay

The recombinant His–FLAG–CPK28 proteins were purified from *E. coli* using Ni-NTA agarose. MBP-ATL31$^{\Delta TM}$/ATL6$^{\Delta TM}$-HA or MBP-HA proteins immobilized on amylose resin (New England BioLabs) were incubated with purified His-tagged recombinant proteins. The incubation was carried out at 4°C for 2 h with gentle shaking. The incubation buffer contained 20-mM Tris–HCl (pH 7.5), 150-mM NaCl, 3-mM EDTA, and 0.5% Triton X-100. The amylose resin was collected and washed five times with buffer containing 20-mM Tris–HCl (pH 7.5), 3-mM EDTA, 150-mM NaCl, and 0.1% Triton X-100. The bound His-tagged proteins were detected by immunoblotting using anti-FLAG antibodies (Sigma).

In vitro ubiquitination assay

The ubiquitination assay using a bacterial reconstituted system was performed as previously described (Han et al.,

2017). The *pCDFDuet-MBP-CPK28/BIK1/BAK1CD-HA-UBA1-S*, *pACYCDuet-ATL31$^{\Delta TM}$/ATL6$^{\Delta TM}$/ATL2$^{\Delta TM}$/PUB25-MYC-UBC8-S*, and *pET28a-FLAG-Ub* plasmids were co-transformed into *E. coli* BL21 (DE3) competent cells. The bacteria were cultured at 37°C in 500-μL liquid Luria-Bertani (LB) medium. When the absorbance at 600 nm reached 0.5, 0.5-mM isopropyl β-D-1-thiogalactopyranoside was applied to induce the expression of recombinant proteins. The bacteria were grown at 28°C for 10 h. Protein ubiquitination was analyzed by immunoblotting with anti-HA, anti-FLAG, and anti-MYC antibodies.

Cell-free protein degradation assay

Total cell-free extracts were obtained from 14-day-old Col-0 or *atl31 alt6* mutant seedlings using protein extraction buffer (50-mM Tris–MES, pH 8.0, 0.5-M sucrose, 1-mM $MgCl_2$, 10-mM EDTA, pH 8.0, 5-mM DTT). Purified recombinant MBP-CPK28-HA proteins were incubated with the above cell-free extracts in the presence of 1-mM ATP, with or without 50-mM MG132 (at 25°C). The degradation of MBP-CPK28-HA proteins was detected by immunoblotting with anti-HA antibodies.

MAPK activation assay

Seven-day-old seedlings were treated with 100-nM flg22 or water. MPK3/6 activation was detected by immunoblotting with anti-pErk1/2 antibodies (Cell Signaling Technology). ACTIN was used as the loading control, which was detected by immunoblotting with anti-beta-ACTIN antibodies (Cell Signal Pathway Research Tools Supplier).

ROS burst assay

ROS production was measured as described previously (Li et al., 2014). Leaf discs (4 mm in diameter) were collected from the leaves of 30-day-old plants. The leaf discs were soaked overnight in sterile water in a 96-well plate. The water was then replaced with ROS measurement solution containing 10-μg·mL^{-1} horseradish peroxidase (Sigma), 50-μM luminol (Sigma), and 100-nM flg22. Luminescence was captured and ROS production was measured immediately using a GLOMAX 96 microplate luminometer (Promega). The values for ROS production are represented by Relative Light Units (RLU), which were determined based on the data obtained from eight leaf discs per treatment.

Stomatal aperture measurement

Stomatal aperture was measured as described by Li et al. (2014) with some modifications. Before flg22 or ABA treatment, 4-week-old plants were kept under the light for 2 h so that most of the stomata were opened. The leaves were collected and soaked in buffer containing 10-mM MES (pH 6.15), 10-mM KCl, and 10-mM $CaCl_2$. The leaves were then treated with 10-μM flg22 or 10-μM ABA for 1 h and the stomata were observed under a light microscope (Leica). Image J software (NIH, Bethesda, MD, USA) was used to measure the stomatal aperture. At least eight peels from eight different plants were examined for each treatment. Number of stomata counted in Figure 8C are: Col-0 mock: n = 144, Col-0 flg22: n = 144, *atl31 atl6* mock: n = 144, *atl31 atl6* flg22: n = 144, *bik1* mock: n = 144, *bik1* flg22: n = 144. Number of stomata counted in Figure 8D are: Col-0 mock: n = 100, Col-0 flg22: n = 100, *atl31 atl6* mock: n = 144, *atl31 atl6* flg22: n = 144, *bik1* mock: n = 144, *bik1* flg22: n = 144.

Pathogen infection assay

Pseudomonas syringae pv. *tomato* (*Pst*) strain DC3000 *COR*$^-$ or DC3000 *hrcC*$^-$ was grown overnight at 28°C in liquid King's B (KB) medium supplemented with 50-μg·mL^{-1} rifampicin. Bacteria were collected by centrifugation (376*g*) at room temperature for 5 min, and washed with H_2O. The bacteria were diluted with H_2O to the desired density (optical density $[OD]_{600}$ = 0.1). Thirty-day-old plants were dipped into 5×10^8 cfu·mL^{-1} *Pst* DC3000 *COR*$^-$ solution containing 0.15% gelatin (Amresco) for 15 s (Jiang et al., 2013), or infiltrated with 5×10^8 cfu·mL^{-1} *Pst* DC3000 *hrcC*$^-$ solution using a needleless syringe. Three-day post inoculation, leaf discs were ground in 100-μL H_2O, and 10-fold serial dilutions of the bacteria solution were prepared to measure bacterial growth. Bacteria were grown on KB plates with 50-μg·mL^{-1} rifampicin at 28°C for 3 days, and bacterial colony forming units were counted.

Statistical analysis

Statistical significance was determined by one-way analysis of variance (ANOVA) and Student's *t* tests; *P*-values were generated using GraphPad Prism 7.04.

Accession numbers

Sequence data from this article can be found in GenBank (https://www.ncbi.nlm.nih.gov/gene/) and the Arabidopsis Information Resource (http://www.arabidopsis.org/) under the following accession numbers: *FLS2*: NP_199445.1, AT5G46330; *BAK1*: NP_567920.1, AT4G33430; *BIK1*: NP_181496.1, AT2G39660; *ATL31*: NP_198094.1, AT5G27420; *ATL6*: NP_566249.1, AT3G05200; *CPK8*: NP_197446.1, AT5G19450; *ATL2*: NP_188294.1, AT3G16720; *BRI1*: NP_195650.1, AT4G39400; *PCRK1*: NP_187594.1, AT3G09830; *PUB25*: NP_566632.1, AT3G19380; *BIR2*: NP_189486.1, AT3G28450; *BIR3*: NP_174039.1, AT1G27190; *PBL13*: NP_198408.2, AT1G27190; *RCN1*: NP_174039.1, AT1G25490; *BSK1*: NP_567980.1, AT4G35230; CPK6: NP_565411.2, AT2G17290; CPK1: NP_196107.1, AT5G04870; CPK3: NP_194096.1, AT4G23650; CPK16: NP_179379.1, AT2G17890. Mutants used in this article can be obtained from ABRC under the following accession numbers: *atl31* (GK_746D08), *atl6* (SALK_149614), *cpk28-1* (WiscDslox246D03), *cpk28-3* (GABI_523B08), *fls2* (SALK_141277), *bak1-4* (SALK_116202), *bik1*(Salk_005291). The RNA-seq data were deposited into National Center for Biotechnology Information and are accessible via BioProject accession number PRJNA742510.

Supplemental data

The following materials are available in the online version of this article.

Supplemental Figure S1. BIR2 and BIR3 undergo ubiquitination.

Supplemental Figure S2. Identification of *cpk28* mutants and verification of the specificity of anti-CPK28 antibodies.

Supplemental Figure S3. Various negative immune regulators undergo proteasomal degradation.

Supplemental Figure S4. Screening of differentially expressed ubiquitin ligase genes upon flg22 treatment.

Supplemental Figure S5. Validation of the feasibility of the protoplast cell-based screening system.

Supplemental Figure S6. Screening of ubiquitin ligases that can potentially mediate CPK28 degradation.

Supplemental Figure S7. ATL31 is localized to the plasma membrane in Arabidopsis protoplasts.

Supplemental Figure S8. Measurement of transcript levels of *ATL31*, *CPK28*, and the *CPK28*-RI splice variant upon flg22 treatment.

Supplemental Figure S9. ATL31 does not associate with CPK8.

Supplemental Figure S10. The CPK28^{G2A} variant loses its plasma membrane localization in protoplasts.

Supplemental Figure S11. Identification of the homozygous T-DNA insertion mutants *atl31 and atl6* and generation of the *atl31 atl6* double mutant.

Supplemental Figure S12. ATL31 promotes the ubiquitination of CPK28.

Supplemental Figure S13. The specificity of CPK28 ubiquitination by ATL31.

Supplemental Figure S14. Overexpressing *ATL31/6* reduces CPK28 protein accumulation in Arabidopsis protoplasts.

Supplemental Figure S15. CPK28 protein accumulation in Col-0, *atl31 atl6*, and *bik1* plants.

Supplemental Figure S16. *CPK28* transcript levels in *atl31 atl6* and Col-0.

Supplemental Figure S17. ATL31 specifically promotes BIK1 protein accumulation in protoplasts.

Supplemental Figure S18. Growth of *Pst* DC3000 *hrcC*$^-$ in *atl31 atl6*, *cpk28-1*, and Col-0 plants.

Supplemental Table S1. The differentially expressed ubiquitin ligase genes upon flg22 treatment.

Supplemental Table S2. Primers used for genotyping, cloning, and RT-qPCR.

Supplemental Table S3. Student' s *t* test tables.

Supplemental Table S4. ANOVA tables.

Acknowledgments

We thank Drs Ping He and Libo Shan (Texas A&M University) for the *bik1*, *fls2*, and *bak1-4* seeds.

Funding

The work was supported by grants from the National Natural Science Foundation of China (32070555, 31800222), the Natural Science Foundation of Hebei Province (C2019503069), and the State Key Laboratory of Plant Genomics.

Conflict of interest statement. The authors declare no conflict of interests.

References

Aguilar-Hernández V, Aguilar-Henonin L, Guzmán P (2011) Diversity in the architecture of ATLs, a family of plant ubiquitin-ligases, leads to recognition and targeting of substrates in different cellular environments. PLoS ONE **6:** e23934

Bazin J, Mariappan K, Jiang Y, Blein T, Voelz R, Crespi M, Hirt H (2020) Role of MPK4 in pathogen-associated molecular pattern-triggered alternative splicing in Arabidopsis. PLoS Pathog **16:** e1008401

Bender KW, Blackburn RK, Monaghan J, Derbyshire P, Menke FL, Zipfel C, Goshe MB, Zielinski RE, Huber SC (2017) Autophosphorylation-based calcium ($Ca2^+$) sensitivity priming and $Ca2^+$/calmodulin inhibition of *Arabidopsis thaliana* $Ca2^+$-dependent Protein Kinase 28 (CPK28). J Biol Chem **292:** 3988–4002

Berrocal-Lobo M, Stone S, Yang X, Antico J, Callis J, Ramonell KM, Somerville S (2010) ATL9, a RING zinc finger protein with E3 ubiquitin ligase activity implicated in chitin- and NADPH oxidase-mediated defense responses. PLoS ONE **5:** e14426

Boudsocq M, Sheen J (2013) CDPKs in immune and stress signaling. Trends Plant Sci **18:** 30–40

Bredow M, Bender KW, Johnson Dingee A, Holmes DR, Thomson A, Ciren D, Tanney CAS, Dunning KE, Trujillo M, Huber SC, et al. (2021). Phosphorylation-dependent subfunctionalization of the calcium-dependent protein kinase CPK28. Proc Natl Acad Sci USA **118:** e2024272118

Bredow M, Monaghan J (2021) Differential regulation of the calcium-dependent protein kinase CPK28 by site-specific modification. Plant Physiol **186:** 1358–1361

Callis J (2014) The ubiquitination machinery of the ubiquitin system. Arab B **12:** e0174

Chevalier D, Morris ER, Walker JC (2009) 14-3-3 and FHA domains mediate phosphoprotein interactions. Annu Rev Plant Biol **60:** 67–91

Chinchilla D, Zipfel C, Robatzek S, Kemmerling B, Nurnberger T, Jones JD, Felix G, Boller T (2007) A flagellin-induced complex of the receptor FLS2 and BAK1 initiates plant defence. Nature **448:** 497–500

Czechowski T, Stitt M, Altmann T, Udvardi MK, Scheible WR (2005) Genome-wide identification and testing of superior reference genes for transcript normalization in Arabidopsis. Plant Physiol **139:** 5–17

Dressano K, Weckwerth PR, Poretsky E, Takahashi Y, Villarreal C, Shen Z, Schroeder JI, Briggs SP, Huffaker A (2020) Dynamic regulation of Pep-induced immunity through post-translational control of defence transcript splicing. Nat Plants **6:** 1008–1019

Furlan G, Nakagami H, Eschen-Lippold L, Jiang X, Majovsky P, Kowarschik K, Hoehenwarter W, Lee J, Trujillo M (2017) Changes in PUB22 ubiquitination modes triggered by MITOGEN-ACTIVATED PROTEIN KINASE3 dampen the immune response. Plant Cell **29:** 726–745

Gómez-Ariza J, Campo S, Rufat M, Estopà M, Messeguer J, San Segundo B, Coca M (2007) Sucrose-mediated priming of plant defense responses and broad-spectrum disease resistance by overexpression of the maize pathogenesis-related PRms protein in rice plants. Mol Plant Microbe Interact **20:** 832–842

Gomez-Gomez L, Boller T (2000) FLS2: an LRR receptor-like kinase involved in the perception of the bacterial elicitor flagellin in Arabidopsis. Mol Cell **5:** 1003–1011

Grubb LE, Derbyshire P, Dunning KE, Zipfel C, Menke FLH, Monaghan J (2021) Large-scale identification of ubiquitination sites on membrane-associated proteins in Arabidopsis thaliana seedlings. Plant Physiol **185:** 1483–1488

Guzmán P (2014) ATLs and BTLs, plant-specific and general eukaryotic structurally-related E3 ubiquitin ligases. Plant Sci **215–216:** 69–75

Halter T, Imkampe J, Mazzotta S, Wierzba M, Postel S, Bücherl C, Kiefer C, Stahl M, Chinchilla D, Wang X, et al. (2014). The leucine-rich repeat receptor kinase BIR2 is a negative regulator of BAK1 in plant immunity. Curr Biol **24:** 134–143

Han Y, Sun J, Yang J, Tan Z, Luo J, Lu D (2017) Reconstitution of the plant ubiquitination cascade in bacteria using a synthetic biology approach. Plant J **91:** 766–776

Heese A, Hann DR, Gimenez-Ibanez S, Jones AM, He K, Li J, Schroeder JI, Peck SC, Rathjen JP (2007) The receptor-like kinase SERK3/BAK1 is a central regulator of innate immunity in plants. Proc Natl Acad Sci USA **104:** 12217–12222

Hegeman AD, Rodriguez M, Han BW, Uno Y, Phillips, GN Jr, Hrabak EM, Cushman JC, Harper JF, Harmon AC, Sussman MR (2006) A phyloproteomic characterization of in vitro autophosphorylation in calcium-dependent protein kinases. Proteomics **6:** 3649–3664

Huang G, Sun J, Bai J, Han Y, Fan F, Wang S, Zhang Y, Zou Y, Han Z, Lu D (2019) Identification of critical cysteine sites in brassinosteroid-insensitive 1 and novel signaling regulators using a transient expression system. New Phytol **222:** 1405–1419

Imkampe J, Halter T, Huang S, Schulze S, Mazzotta S, Schmidt N, Manstretta R, Postel S, Wierzba M, Yang Y, et al. (2017) The Arabidopsis leucine-rich repeat receptor kinase BIR3 negatively regulates BAK1 receptor complex formation and stabilizes BAK1. Plant Cell **29:** 2285–2303

Jiang S, Yao J, Ma KW, Zhou H, Song J, He SY, Ma W (2013) Bacterial effector activates jasmonate signaling by directly targeting JAZ transcriptional repressors. PLoS Pathog **9:** e1003715

Jones JD, Dangl JL (2006) The plant immune system. Nature **444:** 323–329

Kadota Y, Sklenar J, Derbyshire P, Stransfeld L, Asai S, Ntoukakis V, Jones JD, Shirasu K, Menke F, Jones A, et al. (2014). Direct regulation of the NADPH oxidase RBOHD by the PRR-associated kinase BIK1 during plant immunity. Mol Cell **54:** 43–55

Komander D, Rape M (2012) The ubiquitin code. Annu Rev Biochem **81:** 203–229

Kong Q, Sun T, Qu N, Ma J, Li M, Cheng YT, Zhang Q, Wu D, Zhang Z, Zhang Y (2016) Two redundant receptor-like cytoplasmic kinases function downstream of pattern recognition receptors to regulate activation of SA biosynthesis. Plant Physiol **171:** 1344–1354

Kraft E, Stone SL, Ma L, Su N, Gao Y, Lau OS, Deng XW, Callis J (2005) Genome analysis and functional characterization of the E2 and RING-type E3 ligase ubiquitination enzymes of Arabidopsis. Plant Physiol **139:** 1597–1611

Krol E, Mentzel T, Chinchilla D, Boller T, Felix G, Kemmerling B, Postel S, Arents M, Jeworutzki E, Al-Rasheid KA, et al. (2010) Perception of the Arabidopsis danger signal peptide 1 involves the pattern recognition receptor AtPEPR1 and its close homologue AtPEPR2. J Biol Chem **285:** 13471–13479

Lee D, Lal NK, Lin ZD, Ma S, Liu J, Castro B, Toruno T, Dinesh-Kumar SP, Coaker G (2020) Regulation of reactive oxygen species during plant immunity through phosphorylation and ubiquitination of RBOHD. Nat Commun **11:** 1838

Li L, Li M, Yu L, Zhou Z, Liang X, Liu Z, Cai G, Gao L, Zhang X, Wang Y, et al. (2014) The FLS2-associated kinase BIK1 directly phosphorylates the NADPH oxidase RbohD to control plant immunity. Cell Host Microbe **15:** 329–338

Lin ZJ, Liebrand TW, Yadeta KA, Coaker G (2015) PBL13 is a serine/threonine protein kinase that negatively regulates Arabidopsis immune responses. Plant Physiol **169:** 2950–2962

Lozano-Durán R, Bourdais G, He SY, Robatzek S (2014) The bacterial effector HopM1 suppresses PAMP-triggered oxidative burst and stomatal immunity. New Phytol **202:** 259–269

Lu D, Lin W, Gao X, Wu S, Cheng C, Avila J, Heese A, Devarenne TP, He P, Shan L (2011) Direct ubiquitination of pattern recognition receptor FLS2 attenuates plant innate immunity. Science **332:** 1439–1442

Lu D, Wu S, Gao X, Zhang Y, Shan L, He P (2010) A receptor-like cytoplasmic kinase, BIK1, associates with a flagellin receptor complex to initiate plant innate immunity. Proc Natl Acad Sci USA **107:** 496–501

Ma SW, Morris VL, Cuppels DA (1991**)** Characterization of a DNA region required for production of the phytotoxin coronatine by *Pseudomonas syringae* pv. tomato. Mol Plant Microbe Interact **4:** 69–77

Ma X, Claus LAN, Leslie ME, Tao K, Wu Z, Liu J, Yu X, Li B, Zhou J, Savatin DV, et al. (2020). Ligand-induced monoubiquitination of BIK1 regulates plant immunity. Nature **581:** 199–203

Maekawa S, Sato T, Asada Y, Yasuda S, Yoshida M, Chiba Y, Yamaguchi J (2012) The Arabidopsis ubiquitin ligases ATL31 and ATL6 control the defense response as well as the carbon/nitrogen response. Plant Mol Biol **79:** 217–227

Matschi S, Hake K, Herde M, Hause B, Romeis T (2015) The calcium-dependent protein kinase CPK28 regulates development by inducing growth phase-specific, spatially restricted alterations in jasmonic acid levels independent of defense responses in Arabidopsis. Plant Cell **27:** 591–606

Matschi S, Werner S, Schulze WX, Legen J, Hilger HH, Romeis T (2013) Function of calcium-dependent protein kinase CPK28 of *Arabidopsis thaliana* in plant stem elongation and vascular development. Plant J **73:** 883–896

Melotto M, Underwood W, Koczan J, Nomura K, He SY (2006) Plant stomata function in innate immunity against bacterial invasion. Cell **126:** 969–980

Monaghan J, Matschi S, Shorinola O, Rovenich H, Matei A, Segonzac C, Malinovsky FG, Rathjen JP, MacLean D, Romeis T, et al. (2014). The calcium-dependent protein kinase CPK28 buffers plant immunity and regulates BIK1 turnover. Cell Host Microbe **16:** 605–615

Roberts MR, Salinas J, Collinge DB (2002) 14-3-3 proteins and the response to abiotic and biotic stress. Plant Mol Biol **50:** 1031–1039

Ros B, Mohler V, Wenzel G, Thummler F (2008) Phytophthora infestans-triggered response of growth- and defense-related genes in potato cultivars with different levels of resistance under the influence of nitrogen availability. Physiol Plant **133:** 386–396

Roux M, Schwessinger B, Albrecht C, Chinchilla D, Jones A, Holton N, Malinovsky FG, Tor M, de Vries S, Zipfel C (2011) The Arabidopsis leucine-rich repeat receptor-like kinases BAK1/SERK3 and BKK1/SERK4 are required for innate immunity to hemibiotrophic and biotrophic pathogens. Plant Cell **23:** 2440–2455

Sato T, Maekawa S, Yasuda S, Domeki Y, Sueyoshi K, Fujiwara M, Fukao Y, Goto DB, Yamaguchi J (2011) Identification of 14-3-3 proteins as a target of ATL31 ubiquitin ligase, a regulator of the C/N response in Arabidopsis. Plant J **68:** 137–146

Sato T, Maekawa S, Yasuda S, Sonoda Y, Katoh E, Ichikawa T, Nakazawa M, Seki M, Shinozaki K, Matsui M, et al. (2009). CNI1/ATL31, a RING-type ubiquitin ligase that functions in the carbon/nitrogen response for growth phase transition in Arabidopsis seedlings. Plant J **60:** 852–864

Segonzac C, Macho AP, Sanmartin M, Ntoukakis V, Sanchez-Serrano JJ, Zipfel C (2014) Negative control of BAK1 by protein phosphatase 2A during plant innate immunity. EMBO J **33:** 2069–2079

Serrano M, Guzman P (2004) Isolation and gene expression analysis of *Arabidopsis thaliana* mutants with constitutive expression of *ATL2*, an early elicitor-response RING-H2 zinc-finger gene. Genetics **167:** 919–929

Shan L, He P, Li J, Heese A, Peck SC, Nurnberger T, Martin GB, Sheen J (2008) Bacterial effectors target the common signaling partner BAK1 to disrupt multiple MAMP receptor-signaling complexes and impede plant immunity. Cell Host Microbe **4:** 17–27

Stegmann M, Anderson RG, Ichimura K, Pecenkova T, Reuter P, Žársky V, McDowell JM, Shirasu K, Trujillo M (2012) The ubiquitin ligase PUB22 targets a subunit of the exocyst complex required

for PAMP-triggered responses in *Arabidopsis*. Plant Cell **24:** 4703–4716

Stegmann M, Monaghan J, Smakowska-Luzan E, Rovenich H, Lehner A, Holton N, Belkhadir Y, Zipfel C (2017) The receptor kinase FER is a RALF-regulated scaffold controlling plant immune signaling. Science **355:** 287–289

Stewart MD, Ritterhoff T, Klevit RE, Brzovic PS (2016) E2 enzymes: more than just middle men. Cell Res **26:** 423–440

Swatek KN, Wilson RS, Ahsan N, Tritz RL, Thelen JJ (2014) Multisite phosphorylation of 14-3-3 proteins by calcium-dependent protein kinases. Biochem J **459:** 15–25

Thor K, Jiang S, Michard E, George J, Scherzer S, Huang S, Dindas J, Derbyshire P, Leitão N, DeFalco TA, et al. (2020). The calcium-permeable channel OSCA1.3 regulates plant stomatal immunity. Nature **585:** 569–573

Tian W, Hou C, Ren Z, Wang C, Zhao F, Dahlbeck D, Hu S, Zhang L, Niu Q, Li L, et al. (2019) A calmodulin-gated calcium channel links pathogen patterns to plant immunity. Nature **572:** 131–135

Trapnell C, Pachter L, Salzberg SL (2009) TopHat: discovering splice junctions with RNA-Seq. Bioinformatics **25:** 1105–1111

Trujillo M, Ichimura K, Casais C, Shirasu K (2008) Negative regulation of PAMP-triggered immunity by an E3 ubiquitin ligase triplet in Arabidopsis. Curr Biol **18:** 1396–1401

Turek I, Tischer N, Lassig R, Trujillo M (2018) Multi-tiered pairing selectivity between E2 ubiquitin-conjugating enzymes and E3 ligases. J Biol Chem **293:** 16324–16336

Vidal EA, Gutierrez RA (2008) A systems view of nitrogen nutrient and metabolite responses in Arabidopsis. Curr Opin Plant Biol **11:** 521–529

Wang J, Grubb LE, Wang J, Liang X, Li L, Gao C, Ma M, Feng F, Li M, Li L, et al. (2018) A regulatory module controlling homeostasis of a plant immune kinase. Mol Cell **69:** 493–504

Wang ZY, Seto H, Fujioka S, Yoshida S, Chory J (2001) BRI1 is a critical component of a plasma-membrane receptor for plant steroids. Nature **411:** 219

Xu J, Xie J, Yan C, Zou X, Ren D, Zhang S (2014) A chemical genetic approach demonstrates that MPK3/MPK6 activation and NADPH oxidase-mediated oxidative burst are two independent signaling events in plant immunity. Plant J **77:** 222–234

Yamaguchi Y, Huffaker A, Bryan AC, Tax FE, Ryan CA (2010) PEPR2 is a second receptor for the Pep1 and Pep2 peptides and contributes to defense responses in Arabidopsis. Plant Cell **22:** 508–522

Yamaguchi Y, Pearce G, Ryan CA (2006) The cell surface leucine-rich repeat receptor for AtPep1, an endogenous peptide elicitor in Arabidopsis, is functional in transgenic tobacco cells. Proc Natl Acad Sci USA **103:** 10104–10109

Yang X, Wang W, Coleman M, Orgil U, Feng J, Ma X, Ferl R, Turner JG, Xiao S (2009) Arabidopsis 14-3-3 lambda is a positive regulator of RPW8-mediated disease resistance. Plant J **60:** 539–550

Yasuda S, Aoyama S, Hasegawa Y, Sato T, Yamaguchi J (2017) Arabidopsis CBL-interacting protein kinases regulate carbon/nitrogen-nutrient response by phosphorylating ubiquitin ligase ATL31. Mol Plant **10:** 605–618

Zhang J, Li W, Xiang T, Liu Z, Laluk K, Ding X, Zou Y, Gao M, Zhang X, Chen S, et al. (2010) Receptor-like cytoplasmic kinases integrate signaling from multiple plant immune receptors and are targeted by a *Pseudomonas syringae* effector. Cell Host Microbe **7:** 290–301

Zhao Q, Tian M, Li Q, Cui F, Liu L, Yin B, Xie Q (2013) A plant-specific in vitro ubiquitination analysis system. Plant J **74:** 524–533

Zipfel C (2014) Plant pattern-recognition receptors. Trends Immunol **35:** 345–351

Zipfel C, Kunze G, Chinchilla D, Caniard A, Jones JD, Boller T, Felix G (2006) Perception of the bacterial PAMP EF-Tu by the receptor EFR restricts Agrobacterium-mediated transformation. Cell **125:** 749–760

Zou Y, Wang S, Lu D (2020) MiR172b-TOE1/2 module regulates plant innate immunity in an age-dependent manner. Biochem Biophys Res Commun **531:** 503–507

Zou Y, Wang S, Zhou Y, Bai J, Huang G, Liu X, Zhang Y, Tang D, Lu D (2018) Transcriptional regulation of the immune receptor FLS2 controls the ontogeny of plant innate immunity. Plant Cell **30:** 2779–2794